Zootaxa 4613 (2): 201–239
https://www.mapress.com/j/zt/

Article

ISSN 1175-5326 (print edition)
ZOOTAXA
ISSN 1175-5334 (online edition)

https://doi.org/10.11646/zootaxa.4613.2.1
http://zoobank.org/urn:lsid:zoobank.org:pub:A6591BD1-5729-49B2-980B-F1804FE28D3F

Recent thecideide brachiopods from a submarine cave in the Department of Mayotte (France), northern Mozambique Channel

ERIC SIMON[1†], NORTON HILLER[2], ALAN LOGAN[3],
DIMITRI THEUERKAUFF[4,5] & BERNARD MOTTEQUIN[1,6]

[1]*Royal Belgian Institute of Natural Sciences. O.D. Earth and History of Life, Vautier Street 29, B-1000 Brussels, Belgium. E-mail: bmottequin@naturalsciences.be*
[2]*Canterbury Museum, Rolleston Avenue, Christchurch 8013, New Zealand. E-mail: nhiller@canterburymuseum.com*
[3]*Centre for Coastal Studies, University of New Brunswick, Saint-John, N.B., E2L, 4L5, Canada. E-mail: logan@unbsj.ca*
[4]*MR MARBEC (University of Montpellier, CNRS, IFREMER, IRD), Montpellier, France*
[5]*Centre Universitaire de Mayotte, 97660 Dembeni, Mayotte, France. E-mail: dimitri-cz@hotmail.com*
[6]*Corresponding author*
[†]*Deceased on 11 February 2018*

Abstract

For the first time large numbers of thecideide brachiopods have been collected from the Mozambique Channel, more particularly from the western part of the Comorian Island of Mayotte (France). The moderately diverse brachiopod fauna is from a submarine cave situated on the second barrier reef encircling this island, with three different genera being found: *Thecidellina*, *Ospreyella* and *Minutella*. The last genus is represented by *M.* cf. *minuta* (Cooper, 1981), which was first discovered around Madagascar. *Ospreyella* is represented by a new species (*O. mayottensis* **sp. nov.**) as is *Thecidellina,* which is represented by *T. leipnitzae* **sp. nov.** This species is markedly distinct from *T. europa* Logan *et al*., 2015 from Europa Island in the southern Mozambique Channel (1,200 km south of Mayotte), providing an example of allopatric speciation in an isolated cryptic habitat.

Key words: Brachiopoda, *Thecidellina*, *Ospreyella, Minutella,* new species, allopatric speciation, Mozambique Channel

Résumé

Pour la première fois, une grande quantité de brachiopodes thécidéides a été récoltée dans le Canal du Mozambique, en particulier dans la partie occidentale de l'île comorienne de Mayotte (France). Cette faune modérément diversifiée de brachiopodes provient d'une grotte sous-marine développée au sein de la seconde barrière récifale encerclant Mayotte. Elle est variée puisqu'elle comprend trois genres différents : *Thecidellina*, *Ospreyella* et *Minutella*. Ce dernier genre est représenté par *Minutella* cf. *minuta* (Cooper, 1981) qui fut d'ailleurs découverte la première fois près de Madagascar. *Ospreyella* comprend une nouvelle espèce (*O. mayottensis* **sp. nov.**) à l'instar de *Thecidellina* qui est représenté par *T. leipnitzae* **sp. nov.** Cette espèce est clairement distincte de *T. europa* Logan *et al*., 2015. Cette dernière a été découverte à proximité de l'île éponyme située dans le sud du Canal du Mozambique (1200 km au sud de Mayotte) et constitue un exemple de spéciation allopatrique dans un environnement cryptique isolé.

Mots-clefs : Brachiopodes, *Thecidellina, Ospreyella, Minutella*, nouvelles espèces, spéciation allopatrique, Canal du Mozambique

Introduction

Brachiopods from the north-eastern coast of South Africa and from the Mozambique Channel have rarely been collected in the past. The expeditions conducted in the Indian Ocean and adjacent seas explored many areas but the Mozambique Channel (Text-Fig. 1) received scant attention. Muir-Wood (1959) provided a list of all the stations from the Indian Ocean investigated up to that time.

Accepted by D. Lee: 17 Apr. 2019; published: 5 Jun. 2019

During the years 1933–1934 the R.V. Anton Bruun Cruise collected several species of brachiopods from a number of stations in the Mozambique Channel, which were studied by Cooper (1973).

The Benthedi Cruise, in 1977, collected 17 species of brachiopods especially around Mayotte, Glorieuses and Europa islands (Text-Fig. 1) giving a potential list of the brachiopods present in the southern and northern parts of the Mozambique Channel. Zezina (1987) studied the material from this expedition but her paper is mainly a list of species, as complete and detailed descriptions of this material and useful illustrations are sadly missing. For these reasons most of this material needs revision.

Hiller (1986) studied the brachiopod fauna of South African waters and some species found along the eastern coast of South Africa can be found also in the Mozambique Channel.

Finally, the most recent study dealing with brachiopods from southern and northern Madagascar, as well as from off the Mozambique coast, has been published by Bitner & Logan (2016). The material described in this paper was dredged mostly in relatively deep water and more rarely in shallow water stations (Bitner & Logan 2016, pp. 39–41).

Thecideides from the Mozambique Channel area remain poorly investigated. The oldest record is *Lacazella mauritiana* Dall, 1920. Zezina (1987) cited this species from Europa Island and also from Mayotte (Text-Fig. 1). The taxonomic status of this species was discussed further by Logan (2005), Simon & Hoffmann (2013) and Logan *et al*. (2015). Material from Europa Island was assigned by Simon & Hoffmann (2013) to the genus *Ospreyella*. The taxonomic status of *L. mauritiana* awaits the collection of new material from the type station off Mauritius and without a new study it is not possible to refer to this species further at present.

The discovery of many new species of thecideide brachiopods all around the world has greatly improved our knowledge of this order. New genera such as *Pajaudina* Logan, 1988, *Kakanuiella* Lee & Robinson, 2003, *Ospreyella* Lüter & Wörheide (in Lüter *et al.* 2003) and *Minutella* Hoffmann & Lüter, 2010 changed our opinions concerning the diversity among the extant representatives of this order.

Molecular phylogeny studies based on r-DNA, such as those by Cohen *et al*. (1988) and Cohen & Gawthrop (1996), provided comprehensive models of the position of this taxonomical group in the evolution of brachiopods.

Shell ontogeny in thecideide brachiopods was the subject of numerous recent studies, improving our understanding of the development of the brachidium in the different genera. Baker & Carlson (2010) studied the early ontogenetic stages of growth of a Jurassic brachiopod and proposed an explanation for thecideide ancestry. Logan (2005, 2008), Simon & Hoffmann (2013) and Simon *et al*. (2018a) illustrated very detailed ontogenetic accounts for several extant species. The differences between the ontogenies in the genera *Thecidellina* Thomson, 1915, *Minutella* and *Ospreyella* supports their respective taxonomical positions in the subfamilies Thecidellininae and Lacazellinae.

The material collected from Mayotte and studied in this paper expands our knowledge of the fauna from the Mozambique Channel for shallow water stations and from cryptic environments. Enough material was found to understand the ontogenies and to present detailed morphological descriptions for each species. Three genera are identified: *Thecidellina*, *Minutella* and *Ospreyella*. *Minutella* is reported as *M.* cf. *minuta* (Cooper, 1981) originally collected from Samper Bank southeast of Madagascar. The *Thecidellina* species discovered in Mayotte is absolutely different from *T. europa* from Europa Island in the southern part of the Mozambique Channel, providing a new example of allopatric speciation in an isolated cryptic habitat.

For *Ospreyella*, a new species is erected for our specimens from Mayotte as the material collected from Europa Island and considered as *Ospreyella* sp. by Simon & Hoffmann (2013) is slightly different and is mostly represented by younger shells in quite low numbers. Here in Mayotte, the large sample of specimens collected permitted the illustration of the sexual dimorphic structure, detailed morphological characters and different growth stages through ontogeny.

The living brachiopods collected on dead corals, placed in ethanol, give illustrations of the lophophore and some of them are available for future molecular investigations.

Material and methods

The thecideides investigated in this paper have all been collected at a depth of 23 m in a submarine cave situated in the southern part of the “La Passe bateau” channel on the second barrier reef encircling the Comorian Island of Mayotte (Latitude: -12.9776 S, Longitude +44.9827 E). The cave is situated off the south-west coast of the island

(Text-Fig. 1). The entrance of the cave is around 6 m². The width of the cave varies from 3 m to 9 m; its length measures 8 m and its height is variable with a minimum of 3 m and a maximum of 5 m. Numerous crevices of variable length provide a perfect cryptic habitat. The cave has been built entirely by coral development. The walls and ceiling are made of dead corals but not of local rocks, so this cave is exclusively a biogenic reefal construction. The luminosity inside the cave is rather weak because its entrance is placed horizontally.

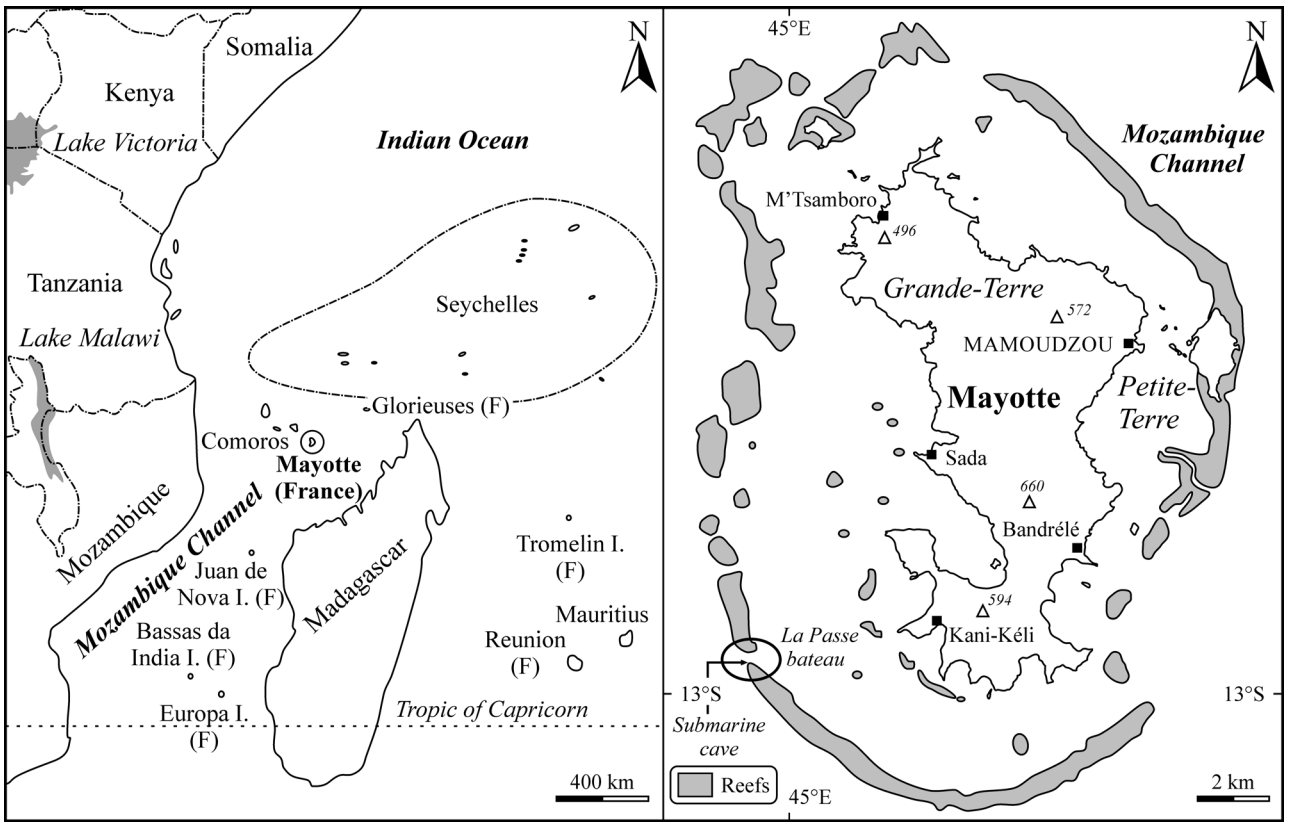

TEXT-FIGURE 1. Schematic localization map of the Island of Mayotte (Department of Mayotte, France) in the context of the Mozambique Channel and localization of the submarine cave situated off the south-western part of the island at the level of its second reef circling wall. The place is called "La Passe bateau" and the cave is situated on the internal side of the reef at a depth of 23 m.

Currents around the cave can be very strong but it is very protected and the material inside the cave is not too much disturbed. Nevertheless, water movements affect the quality of the much more fragile juvenile shells.

Specimen material was collected in June 2016. Samples of the dead coral walls were collected and directly preserved in ethanol at 70%. This material provides and preserves brachiopod specimens for study of their soft tissues in order to investigate the ontogeny of the lophophore and obtaining DNA samples for future molecular studies. However, the bulk of the material collected constituted sediments from the cave floor, which were dried at 40°C in a thermostatic chamber. The dried samples were then sieved using a set of sieves with different meshes, the largest being sized at 2 mm and the smallest at 0.2 mm. Brachiopods were picked out under a binocular microscope, so it was possible to collect all the shells necessary for studying the ontogeny of the different species found. The shells were washed and, when possible, more deeply cleaned using an ultrasonic bath (sometimes when the brachidium is too fragile, the use of the ultrasonic bath was avoided).

Shells of specimens selected for scanning electron microscopy (SEM) were treated with household bleach hypochlorite (at 5%) in order to remove all remaining soft body parts. Several fresh brachiopods preserved in ethanol were critical point dried by passing them through successive ethanol/formaldehyde dimethyl-acetal treatments (respectively 100/0 – 75/25 – 25/75 – 0/100 in %). All samples for SEM were mounted on stubs, sputter coated with gold, and investigated using a low vacuum SEM (ESEM FEI Quanta 200).

Specimens illustrated in this paper are deposited in Paris at the Muséum national d'Histoire naturelle (prefixed MNHN-IB) and are part of the Recent invertebrate collections (brachiopod section).

Taxonomy

Suprafamilial classification follows Williams *et al*. (1996) and the hierarchy within the superfamily Thecideoidea follows Baker (2006). Terminology for the morphological descriptions of the thecidellinid genera *Thecidellina* and *Minutella* follows Hoffmann & Lüter (2009, fig. 2) whereas for the lacazellinine genus *Ospreyella*, it follows Hoffmann *et al*. (2009). Text-Fig. 2 shows some terms of the dorsal internal morphology of these brachiopods that are sometimes named differently by other authors. This paper follows Recommendation 13B of the International Code for Zoological Nomenclature related to language (4th edition, 1999). Abstract and diagnoses in French have been added.

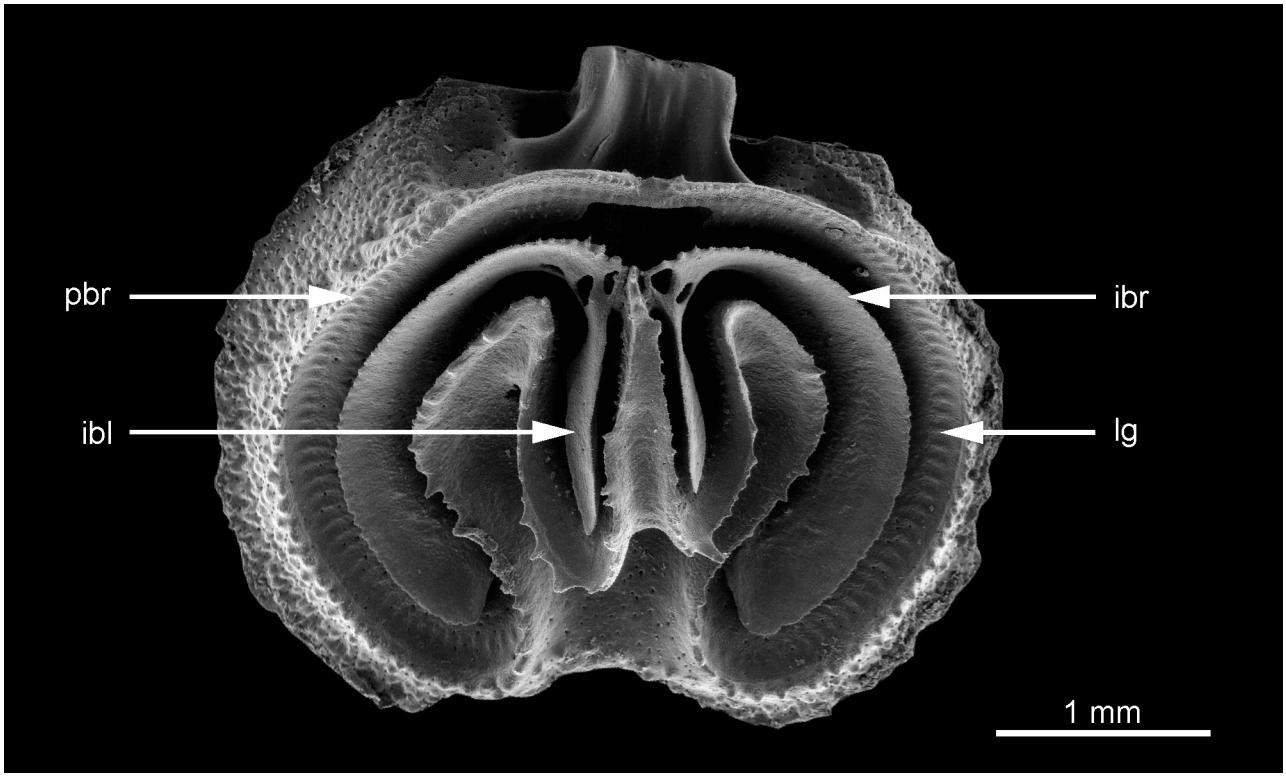

TEXT-FIGURE 2. Precisions on some dorsal internal terms used for the thecideoid brachiopods (*Ospreyella mayottensis* **sp. nov.**, MNHN-IB-2017-179). Abbreviations: ibl, interbrachial lobe, i.e. the lobes occurring between the main arms of the lophophore in *Ospreyella* in particular; ibr, intrabrachial ridge, i.e. the ridges immediately within the main arms of the lophophore and which define the brachial lobes; lg, lophophore groove, i.e. the groove that accommodates the main arms of the lophophore; pbr, peribrachial ridge, i.e. the ridge that encloses the outer margins of the main arms of the lophophore.

PHYLUM BRACHIOPODA DUMÉRIL, 1805

SUBPHYLUM RHYNCHONELLIFORMEA WILLIAMS *ET AL.*, 1996

CLASS RHYNCHONELLATA WILLIAMS *ET AL.*, 1996

ORDER THECIDEIDA ELLIOTT, 1958

SUPERFAMILY THECIDEOIDEA GRAY, 1840

FAMILY THECIDELLINIDAE ELLIOTT, 1958

SUBFAMILY THECIDELLININAE ELLIOTT, 1953

Genus *Thecidellina* Thomson, 1915

Type species. *Thecidium barretti* Davidson, 1864 by original designation.

Thecidellina leipnitzae Simon, Hiller, Logan & Mottequin sp. nov.

Table 1; Text-Fig. 3; Pl. 1, Figs. 1–5; Pl. 2, Figs. 1–3; Pl. 3, Figs. 1–5

Holotype. MNHN-IB-2017-162 (Pl. 2, Fig. 1), a fully-grown adult dorsal specimen opened for observation of the internal structures.

Paratypes. MNHN-IB-2017-159 (Pl. 1, Fig. 3), MNHN-IB-2017-157 (Pl. 1, Fig. 1), MNHN-IB-2017-158 (Pl. 1, Fig. 2), and MNHN-IB-2017-160 (Pl. 1, Fig. 4): complete articulated specimens. MNHN-IB-2017-163 (Pl. 2, Fig. 2), MNHN-IB-2017-164 (Pl. 2, Fig. 3), and MNHN-IB-2017-161 (Pl. 1, Fig. 5): complete specimens opened for the study of internal structures. MNHN-IB-2017-166 (Pl. 3, Fig. 2), MNHN-IB-2017-165 (Pl. 3, Fig. 1), MNHN-IB-2017-168 (Pl. 3, Fig. 4), MNHN-IB-2017-169 (Pl. 3, Fig. 5), and MNHN-IB-2017-167 (Pl. 3, Fig. 3): juvenile complete specimens used for the study of the ontogeny of the brachidium. Morphometric measurements of the holotype and paratypes are indicated in Table 1.

Etymology. The species is dedicated to Heilwig Leipnitz (Uelzen, Germany) in acknowledgement of her constant help by giving us, as often as possible, very interesting brachiopod material for sustaining our studies.

Type locality. Department of Mayotte (France). Submarine cave at 23 m depth situated at La Passe bateau off the south-west coast of the island of Mayotte in the second coral reef barrier (latitude: -12.9776 S, longitude: +44.9827 E).

Additional material. Collected from the sieved sediment of the submarine cave: 435 complete articulated shells, 425 isolated dorsal valves and 136 isolated ventral valves. Living specimens collected from the rocks from the ceiling of the cave: nine specimens placed immediately in ethanol for further DNA studies.

Diagnosis. Small-sized *Thecidellina* species, subtriangular to drop-like in outline. Flat, triangular planodeltidium with densely striated surface. Hemispondylium made of two subparallel prongs anteriorly ended by two curved pointed edges. Ventral valve floor without median ridge and covered with very rough tubercles except in the gonad pits, which have a smooth surface. Lateral ventral valve floor covered with regular subparallel rows of cup-like tubercles. Cyrtomatodont teeth short, blunt. Lid-like slightly convex dorsal valve with prominent protegulum. Very wide, thick dorsal septum with flat ventral surface. Brachial bridge and peribrachial ridge connected by two posterior outgrowths to the intrabrachial ridge. Calcitic pole variable but generally thick. Intrabrachial ridge oval, regular with smooth margins. Brachial cavities or brood pouches in adults partly covered by radially disposed, irregular spicules leaving a free space between each, rarely cemented together in their anterior part. No real canopies over the brachial cavities are observed in this species.

Diagnose. *Thecidellina* de petite taille, subtriangulaire ou en forme de goutte. Le planodeltidium est triangulaire, plat avec une surface nettement striée. L'hémispondylium est constitué de branches subparallèles se terminant par un apex pointu recourbé. La surface de la valve ventrale n'a pas de sillon médian et est couverte de tubercules très rugueux et irréguliers à l'exception des cavités où sont situées les gonades. Les flancs internes latéraux de la valve ventrale sont ornementés de séries parallèles de petits tubercules en forme de ventouses. Les dents sont courtes, robustes avec un apex arrondi. La valve dorsale ressemble à un couvercle faiblement convexe avec un protégulum bien individualisé et proéminent. La valve dorsale a un septum très large et épais dont la surface ventrale est plate. Le pont brachial et la crête intrabrachiale sont reliés par de fortes expansions postérieures. Le pôle calcitique est épais. Cavités brachiales partiellement couvertes par des spicules radialement disposées, assez irrégulières et très rarement cimentées entre elles dans la partie intérieure. Les cavités brachiales ne sont jamais totalement couvertes dans cette espèce.

Description. External shell characters. Small-sized, whitish to light brown thecideide brachiopod (Table 1), with endopunctate shell, generally with drop-like outline in adult stage (Pl. 1, Figs. 1a, 2a, 3a, 4a). The relationships between different ratios, such as length/width and width, length of dorsal valve/width and width, thickness/width and width, and length of hinge line/width and width, are illustrated in Text-Fig. 3. The external surface of the ventral valve is marked by many growth lines of variable thickness (Pl. 1, Figs. 1c, 4c). On the surface of the dorsal valve, which is quite irregular, growth lines are difficult to observe (Pl. 1, Figs. 1a, 2a, 3a, 4a).

TABLE 1. *Thecidellina leipnitzae* **sp. nov.** Morphometric measurements were taken for the holotype, the paratypes and a large number of articulated specimens collected from the sieved sediment collected in the submarine cave in Mayotte at 23 m depth. Abbreviations: N, number of specimens measured; MIN, minimum; MAX, maximum; L, length, W, width; LD, length of dorsal valve; Lint, length of the interarea; Wint, width of the hinge or interarea; T, thickness; nm, value not measured.

Illustrated specimens	**L**	**W**	**LDV**	**Lint**	**Wint**	**T (max)**	**L/W**	**LDV/W**	**Lint/W**	**Wint/W**	**T/W**
	mm	**mm**	**mm**	**mm**	**mm**	**mm**					
Holotype MNHN-IB-2017-162	nm	2.7	3.1	0.75	nm	nm		1.14			
Paratype MNHN-IB-2017-157	3.7	3.1	2.9	1.0	1.5	3.7	1.2	0.9	0.3	0.5	1.2
Paratype MNHN-IB-2017-158	3.2	2.7	2.6	0.7	1.6	1.6	1.2	0.9	0.2	0.6	0.6
Paratype MNHN-IB-2017-159	3.1	2.6	2.4	0.7	1.2	1.5	1.2	0.9	0.3	0.5	0.6
Paratype MNHN-IB-2017-160	2.7	2.4	2.2	0.5	1.2	1.7	1.1	0.9	0.2	0.5	0.7
Paratype MNHN-IB-2017-161	2.9	2.9	2.3	0.6	1.5	1.6	1.0	0.8	0.2	0.5	0.6
Paratype MNHN-IB-2017-163	nm	2.8	2.6	nm	1.6	nm		0.9		0.6	
Paratype MNHN-IB-2017-164	3.0	2.7	2.6	0.4	1.4	nm	1.1	1.0	0.2	0.5	
Paratype MNHN-IB-2017-165	nm	1.0	1.1	nm	0.5	nm		1.1		0.5	
Paratype MNHN-IB-2017-166	nm	1.9	1.8	nn	0.8	nm		0.9		0.4	
Paratype MNHN-IB-2017-167	nm	1.9	1.8	nm	0.8	nm		1.0		0.4	
Paratype MNHN-IB-2017-168	nm	2.2	2.1	nm	1.0	nm		1.0		0.5	
Paratype MNHN-IB-2017-169	nm	2.1	1.9	nm	1.0	nm		0.9		0.5	
Total measurements											
N	45	54	54	46	53	44	45	54	45	53	44
Mean value	2.0	1.0	1.1	0.1	0.5	0.6	0.94	0.74	0.05	0.36	0.30
MIN	4.3	3.4	3.2	1.2	2.2	3.7	1.67	1.33	0.43	0.83	1.19
MAX	3.4	2.7	2.5	0.8	1.5	1.8	1.17	0.92	0.26	0.53	0.62
Standard deviation	0.3858	0.4391	0.3696	0.2357	0.3264	0.5338	0.1448	0.1143	0.0773	0.0979	0.1831
Standard error (±)	0.0575	0.0598	0.0503	0.0348	0.0448	0.0805	0.0216	0.0156	0.0115	0.0134	0.0276

The shell is strongly ventri-biconvex, with the maximum thickness often situated at the anterior part because the growth of the ventral valve is always more important anteriorly (Pl. 1, Fig. 1b). For the dorsal valve, the maximum thickness corresponds to the position of the protegulum (Pl. 1, Figs. 2b, 3c, 4e). The lateral commissure is generally straight or very slightly concave (Pl. 1, Figs. 1b, 3b). The anterior commissure is rectimarginate (Pl. 1, Fig. 1c) or, rarely, slightly sulcate.

The deep ventral valve has a quite variable development. The thickness of the shell is the most variable morphological character (Table 1). The ventral valve is cemented to the substrate by a large portion of its ventral side. The adult shell is often lifted from the substrate anteriorly (Pl. 1, Fig. 1b), its anterior part tending to be always more elevated than its posterior part. Such a development of the ventral valve is common in thecideide brachiopods as already illustrated by Pajaud (1970, p. 219, fig. 130A). During growth, the ventral valve covers all the relief irregularities present on the substrate. A very irregular aspect of the ventral exterior of the shell results from this type of growth.

The interarea is a planodeltidium (Logan & Baker 2013) with an isosceles triangular outline and a flat (Pl. 1, Figs. 1b, 4c) or slightly concave surface (Pl. 1, Fig. 3b–c). The surface of the interarea is densely striated with parallel growth lines. The interarea represents 22–27% of the length of the shell (Table 1). The planodeltidium is straight but can be curved to the left or the right sides (Pl. 1, Fig. 1a) depending on variable habitat conditions. The hinge line is straight without a notch. The interarea and the dorsal valve form a very variable angle at the level of the hinge line (Pl. 1, Fig. 4d).

The lid-like dorsal valve is much smaller than the ventral valve, with a subcircular to elongate oval outline. The weak convexity of this valve culminates posteriorly with the protegulum. The surface of the dorsal valve is quite irregular and growth lines are difficult to observe. The protegulum is subcircular, always very distinct and its external surface is covered with microgranular ornamentation (Pl. 1, Figs. 2b, 4e).

Internal shell characters. The opened ventral valve has a suboval outline (Pl. 1, Fig. 5f; Pl. 2, Figs. 1g, 3). A very narrow, concave and smooth peripheral rim is developed all along the commissure (Pl. 2, Fig. 1g). Along the internal side of this rim, a subperipheral ridge with tubercles is developed. The tubercles are slightly larger posteriorly than in the anterior part of the valve (Pl. 2, Fig. 1g).

The ventral valve floor, without a differentiated median ridge, is very roughly tuberculate with tubercles variable in outline: sometimes the tubercles are like isolated thick spines (Pl. 1, Fig. 5f), sometimes they are grouped by pairs (Pl. 2, Fig. 1g) or they can be irregularly elongate (Pl. 2, Fig. 3). The floor inside the two oval gonad pits is smooth (Pl. 2, Figs. 1g, 3). The gonad pits are very deep in this species and their length attains 30–35% of internal valve length (Pl. 2, Figs. 1g, 3). The endopunctation has a weak density between the tubercles of the valve floor but it increases in the bottom of the gonad pits (Pl. 2, Figs. 1g, 3).

The hemispondylium is made of two parallel, narrow prongs, with pointed curved tips, attached to the posterior part of the valve. The prongs are not very long in this species. Subtriangular to semicircular lateral adductor muscle scars are developed on either side of the hemispondylium and teeth (Pl. 2, Fig. 1g). Teeth are cyrtomatodont, robust, short, blunt and covered with secondary shell material (Pl. 2, Fig. 3).

In the dorsal valve interior, a flat relatively narrow, smooth marginal flange is visible along the commissure (Pl. 1, Fig. 5a). This flange is heavily endopunctate.

The external side of the peribrachial ridge is ornamented with small regular tubercles (Pl. 2, Fig. 1c) and its crest shows also more irregular tubercles till its junction with the brachial bridge (Pl. 2, Figs. 1b–c). A clearly defined peripheral rim is not present. The brachial bridge is moderately elevated and its ventral edge is ornamented with regular small indentations (Pl. 1, Fig. 5a).

In lateral profile the internal structures are weakly raised towards the posterior part (Pl. 1, Fig. 5c; Pl. 2, Fig. 1b) but this character is quite discrete. The median septum is obviously straight, very wide and very thick all along its length. It becomes broader in its anterior part. In its posterior part the septum has a pointed tip (Pl. 1, Fig. 5a; Pl. 2, Figs. 2a, e–f, 2c). In lateral view the median septum has a flat ventral profile. Its ventral surface or edge is granulated (Pl. 2, Figs. 2b, 2e).

There is a smooth lophophore groove between the peribrachial ridge and the intrabrachial ridge. This groove is heavily endopunctate (Pl. 1, Fig. 5a; Pl. 2, Figs. 1a, 2a–b).

The intrabrachial ridge is clearly defined with an oval regular outline and smooth external margins (Pl. 1, Fig. 5a). It is thin and sometimes its thickness is so reduced that the spicules of the brachial cavities are directly visible laterally (Pl. 1, Fig. 5a-c). Marsupial orifices (*sensu* Zumwalt 1970) are situated in the posterior part of the intrabra-

chial ridge, on either side of the septum tip (Pl. 1, Fig. 5a–b; Pl. 2, Figs. 1c, 2c). These orifices are small sub-circular rings (Pl. 2, Fig. 1a, 1c) protected by a relatively thick ventral side (Pl. 2, Figs. 1f, 2c). In the posterior part of the valve, two medium-sized lateral visceral gaps are situated between the intrabrachial ridge and the brachial bridge (Pl. 1, Fig. 5a, 5d; Pl. 2, Figs. 1a–b, 2a, 2c). The central posterior visceral gap between the brachial bridge and the intrabrachial ridge is relatively narrow (Pl. 1, Fig. 5e; Pl. 2, Figs. 1d, 2c).

The brachial bridge has a finely denticulate ventral crest (Pl. 1, Fig. 5d; Pl. 2, Fig. 1a). Clearly defined, strong, wide posterior outgrowths firmly connect the inner side of the brachial bridge and the posterior side of the intrabrachial ridge in adult specimens (Pl. 2, Fig. 2a).

The cardinal process is quite short, trilobate and relatively straight (Pl. 1, Fig. 5a, 5c). At the posterior part of the cardinal process, the diductor muscle scars are quite small (Pl. 1, Fig. 5d). Inner socket ridges are thickened and quite strong. Outer socket ridges are flat and thin. The sockets are deep. Placed on either side of the base of the inner socket ridges, the lateral adductor muscle scars are widely developed (Pl. 1, Fig. 5e).

The calcitic pole is thick and wide ventrally (Pl. 1, Fig. 5e). Seen in posterior view, it is fused with the dorsal valve floor.

The brachial cavities (brood pouches in female specimens) are ovoid, deep and partly covered with single massive canopying spicules. These spicules are relatively thin but quite high, irregular in shape and radially disposed, leaving between them a free space that has always the same size. These spicules do not fuse together and a complete closed canopy is never observed.

Comparison with other species of *Thecidellina*. To make comparisons between *Thecidellina* species it is essential to use material described accurately and well-illustrated (Simon *et al.* 2018a). Specimens collected from their type area are best; care must be taken with material found elsewhere, often at very far distances from the type locality. Determination of *Thecidellina* species is not always easy and a lot of confusion between species is found in the literature. Lee & Robinson (2003) pointed out this problem, having observed "a very wide overlapping" of distribution areas for different Pacific species in the literature. This wide zoogeographical overlapping is surprising in a genus like *Thecidellina* in which cryptic, allopatric speciation processes have been demonstrated (Lüter *et al.* 2008).

The essential comparisons should be made between *T. leipnitzae* **sp. nov.** and other Indo-Pacific species that have a similar structure of brachial cavities. Species that have a completely fused spicular canopy can be directly distinguished. Indeed, in *T. leipnitzae* there is no complete canopy covering brachial cavities and radial spicules develop a characteristic openwork protection for embryos. Species like *T. blochmanni* Dall, 1920 and *T. europa* Logan *et al.*, 2015 develop a complete spicular canopy and can be easily discarded even if the type of canopy is clearly different for each species cited. *T. europa* is found in the southern part of the Mozambique Channel and is distinct from *T. leipnitzae* **sp. nov.** This case further illustrates the clear propensity for the development of allopatric cryptic speciation mechanisms in *Thecidellina* (Lüter *et al*. 2008).

Thecidellina congregata Cooper, 1954 from Bikini Atoll has brachial cavities incompletely covered by a canopy. The cavities are protected by subparallel spicules developed along their external margins. These spicules are of two orders: from the anterior to the middle of the valve the spicules are very thick. From the middle of the valve to the posterior part the spicules are much smaller. There are no spicules along the internal margins of the brachial cavities. However, flanges are developed along the posterior part of the internal margins. The internal side of the peripheral rim has a regular beaded ornamentation. The septum is quite narrow with a concave ventral sulcus. Posteriorly, it is limited by a small circular visceral gap (see Cooper 1954, pl. 80, figs. 9–13). The shell of *T. leipnitzae* **sp. nov.** has brachial cavities covered only with radial spicules but these are of regular size all along the external margins of the brachial cavities (Pl. 2, Fig. 1a). There are no flanges developed along the inner margins of the brachial cavities: the lateral sides of the dorsal septum remain smooth (Pl. 1, Fig. 5a; Pl. 2, Fig. 1a). The internal margin of the peribrachial ridge is not beaded. The septum is much stronger, flat ventrally with a smooth surface and posteriorly it is limited by a larger visceral cavity, which is not circular.

In *Thecidellina maxima* (Hedley, 1899) the anterior commissure is quite emarginate and the ventral valve floor is smoother with small disseminated tubercles. Flanges are developed along the inner margins of the brachial cavities and some spicules can even be developed on that side. The septum is concave ventrally and narrow. In *T. leipnitzae* **sp. nov.** the anterior commissure is rectimarginate. The ventral valve floor is very roughly covered with strong irregular tubercles. The spicules on the brachial cavities are more spaced with a regular size and more radial. There are no flanges along the inner margins of brachial cavities. The septum is wider, thicker and its ventral edge is flat and smooth.

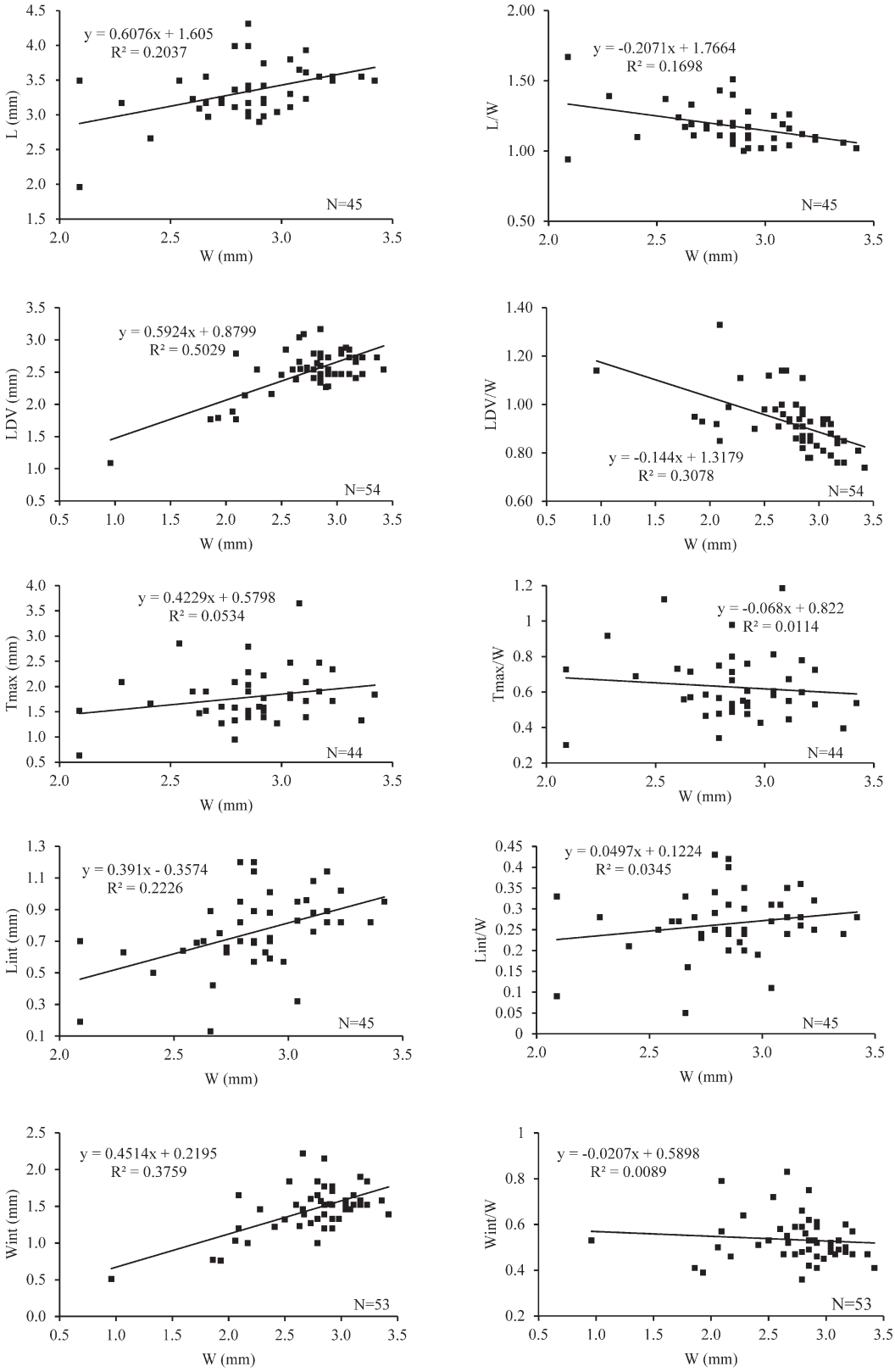

TEXT-FIGURE 3. Scatterplots of morphometric measurements of *Thecidellina leipnitzae* **sp. nov.** Abbreviations: L, length; W, width; LDV, length of dorsal valve; T (max), maximal thickness; Lint, length of the interarea, Wint, width of hinge line or interarea. Relationships between ratios L/W and width, LDV/W and width, T(max)/W and width, Lint/W and width and Wint/W and width. Linear regression and regression coefficient (R^2) indicated. The regression coefficient (R^2) is indicated. N is the number of specimens measured.

The material studied for *Thecidellina insolita* Hoffmann *et al.*, 2009 is abundant. The calcitic pole in this species is not fused with the dorsal valve floor as it is in *T. leipnitzae* **sp. nov.** The cardinal process is more developed and less curved with a strongly developed median ridge. In *T. leipnitzae* **sp. nov.** the cardinal process is shorter and the median ridge is less developed. The canopying spicules in *T. insolita* are single and with a quite regular outline, and they are shorter (Hoffmann *et al*. 2009, fig. 2m). In *T. leipnitzae* **sp. nov.** the spicules have an irregular outline with tuberculate ornamentation on their ventral edge (Pl. 2, Fig. 1e). The posterior visceral gap is larger in *T. insolita* and the posterior outgrowths connecting the brachial bridge to the intrabrachial ridge are widely separated and they have a relatively weak development (Hoffmann *et al*. 2009, fig. 2a, 2i). In *T. leipnitzae* **sp. nov.** posterior outgrowths are strongly developed and they are placed nearer each other (Pl. 1, Fig. 5a, 5d; Pl. 2, Figs. 1a, 1b, 2a). The posterior visceral gap is thus reduced. Both species have a similar dorsal septum which is however flatter in *T. leipnitzae* **sp. nov.** and both possess cup-like tubercles on the peribrachial ridge (defined as "crater-like tubercles" by Hoffmann *et al*. 2009).

In *Thecidellina japonica* (Hayasaka, 1938) the dorsal septum is narrower, more ventrally concave and flares much more in its anterior part. The spicules of the brachial pouches are more fused together and they are shorter. The ventral valve of *T. japonica* has a ventral valve floor with a peculiar median ridge made of three longitudinal series of irregular small tubercles (see Hayasaka 1938, fig. 2b). In *T. leipnitzae* **sp. nov.** the dorsal septum is wider, less flaring in its anterior part and has a flat ventral surface. The spicules of the canopy are more developed, single and cover more of the brachial cavities. The ventral valve floor in *T. leipnitzae* **sp. nov.** is roughly tuberculate and does not develop a median ridge (Pl. 2, Fig. 1g).

Thecidellina mawaliana Simon *et al.*, 2018a has a high, thin dorsal median septum with an acute posterior tip. Its ventral edge is convex and tuberculate or spinous. The brachial cavities are covered by thin, fragile, irregular canopying spicules that become fused during ontogeny but always leaving random gaps. The canopy apparently never completely covers the brood pouches. In *T. leipnitzae* the dorsal septum is much wider with a flat ventral surface that is smooth to granulose. The spicules in the brachial canopy are regularly radially arranged with free space separating them so that a complete canopy is never formed. In addition, the floor of the ventral valve of *T. leipnitzae* is much more coarsely tuberculate than that of *T. mawaliana*.

Shell ontogeny. Shell ontogeny in the genus *Thecidellina* has already been studied and illustrated for different species, e.g. *T. congregata* Cooper, 1954 by Logan (2008), *T. meyeri* Hoffmann & Lüter, 2009, and *T. mawaliana* Simon et al., 2018a. Most of the early juvenile stages of growth are quite similar in the different species. In the ventral valve the teeth, the hemispondylium and the flat interarea are immediately developed. In the earliest dorsal valve, the peribrachial ridge, the brachial bridge and the cardinal process are already developed.

A bifid spike emerges in the central part of the valve with its tips oriented posteriorly. For *T. leipnitzae* **sp. nov.**, the main steps of the ontogeny described and illustrated in Pl. 3, Figs. 1–5 give a comprehensive view of the development. A peculiar aspect of the ontogeny in this species is the fact that when the intrabrachial ridge is emerging in its posterior part, the dispersed tubercles serving as basement for the construction of the whole intrabrachial ridge are not clearly developed as is the case for other species such as the new species described by Simon *et al*. (2018a). These tubercles are produced at a later stage of growth. At this early stage of growth, they are similar to dispersed nodules (Pl. 3, Fig. 1a–c). However, the septum is already emerging and connected with the base of the initial spikes (Pl. 3, Fig. 1b–c). The calcitic pole is undeveloped. Nonetheless a rudimentary median lobe is already visible on the cardinal process.

Later, the posterior part of the intrabrachial ridge develops and progresses anteriorly (Pl. 3, Fig. 2a). The median septum grows rapidly, increasing its height and its width (Pl. 3, Fig. 2a–b). The calcitic pole is now developed and joins the base of the median lobe of the cardinal process (Pl. 3, Fig. 2a–b).

At the next stage of growth, the brachial cavities appear as separated expansions (Pl. 3, Fig. 3a). The septum is stronger. Its ventral edge is now slightly less concave. In the posterior part, small outgrowths appear. They emerge from the base of the brachial bridge as two small pointed nodules (Pl. 3, Fig. 3b). The calcitic pole is now fused with the dorsal valve floor in front of the base of the median lobe of the cardinal process (Pl. 3, Fig. 3b).

Later, the septum reaches its mature form and it is now wide, thick and straight with a pointed posterior tip (Pl. 3, Fig. 4a). The posterior outgrowths fuse the anterior part of the brachial bridge with the posterior part of the intrabrachial ridge (Pl. 3, Fig. 4a, 4c). The calcitic pole and the base of the median lobe of the cardinal process are not fused together (Pl. 3, Fig. 4a). The intrabrachial ridge is now completely erected posteriorly and laterally but its anterior part is still missing. Canopying spicules are now appearing (Pl. 3, Fig. 4a–c). Marsupial orifices are developed at this stage of growth.

Finally, the anterior part of the intrabrachial ridge is erected. Canopying spicules are built all over the brachial cavities except in their posterior part (Pl. 3, Fig. 5a). A remarkable aspect in the ontogeny is the intrabrachial ridge, which is progressively made by erecting separate plates. At the ultimate stage of growth (Pl. 3, Figs. 4a, 5a) these separated plates are fused together.

SUBFAMILY MINUTELLINAE LOGAN & BAKER, 2013

Genus *Minutella* Hoffmann & Lüter, 2010

Type species. *Minutella tristani* Hoffmann & Lüter, 2010, by original designation.

Minutella cf. *minuta* (Cooper, 1981)

Table 2; Text-Figs. 4–5; Pl. 4, Figs. 1–3

cf.	1981	*Thecidellina minuta* new species: Cooper, p. 62, pl. 6, figs. 27–40.
cf.	1985	*Thecidellina minuta* Cooper: Zezina, p. 209.
cf.	1994	*Thecidellina minuta* Cooper: Zezina, p. 50, fig. 3.
cf.	2003	*Thecidellina minuta* Cooper: Lee & Robinson, p. 355.
cf.	2009	*Thecidellina minuta* Cooper, 1981: Bitner, p.18, figs. 13A–I.
cf.	2010	*Thecidellina minuta* Cooper, 1981: Bitner, pp. 653–654, fig. 5A–F.
cf.	2010	*Minutella minuta* (Cooper, 1981): Hoffmann & Lüter, p.148, pl. 2, figs. 13–18, pl. 3, figs. 13–15.
?	2010	*Minutella* cf. *minuta*: Hoffmann & Lüter, pp. 150–152.
?	2013	*Minutella* cf. *minuta*: Simon & Hoffmann, p. 405, pl. 1, figs 1–5, pl. 2, figs. 1–8.
?	2018a	*Minutella* cf. *minuta* (Lembeh form): Simon *et al*.: pp. 495–496, text-fig. 2, pl. 7, figs. 1a–g, 2.

Material illustrated. MNHN-IB-2017-170 (Pl. 4, Fig. 1): complete articulated specimen relatively longer than wide. MNHN-IB-2017-171 (Pl. 4, Fig. 2): complete articulated specimen much wider with a subcircular outline. MNHN-IB-2017-173 (Text-Fig. 4.1): complete articulated, but opened juvenile specimen. MNHN-IB-2017-172 (Pl. 4, Fig. 3): dorsal valve with some posterior part of the spicular canopy preserved. MNHN-IB-2017-174 (Text-Fig. 4.2): adult dorsal valve with partial spicular canopy visible. MNHN-IB-2017-175 (Text-Fig. 4.3): dorsal valve showing a later juvenile stage of growth. MNHN-IB-2017-176 (Text-Fig. 4.4): a dorsal valve with the beginning of the construction of brachial cavities. The calcitic pole is present and the posterior outgrowths between brachial bridge and peribrachial ridge are clearly visible. MNHN-IB-2017-177 (Text-Fig. 5.1) and MNHN-IB-2017-178 (Text-Fig. 5.2): small and larger adult specimens showing the brachial cavity covered with a membrane. Morphometric measurements of the illustrated material are indicated in Table 2.

TABLE 2. *Minutella* cf. *minuta* (Cooper, 1981). Morphometric measurements were taken for the specimens illustrated in this paper. This material has been extracted from the sieved sediment collected in a submarine cave in Mayotte at 23 m depth. Abbreviations: L, length; W, width; LDV, length of dorsal valve; Lint, length of the interarea; Wint, width of the hinge or interarea; T, thickness; nm, value not measured.

Specimens	L	W	LDV	Lint	Wint	T (max)	L/W	LDV/W	Lint/W	Wint/W	T/W
MNHN-IB	mm	mm	mm	mm	mm	mm					
2017-170	2.1	1.4	1.5	0.6	0.7	1.1	1.44	1.05	0.39	0.48	0.76
2017-171	2.0	1.7	1.6	0.4	0.8	nm	1.17	0.93	0.24	0.42	
2017-172	2.0	1.5	1.5	0.5	0.6	nm	1.33	1.01	0.32	0.39	
2017-173	0.7	0.8	0.8	0.1	0.5	0.5	0.94	0.51	0.09	0.60	0.69
2017-174	nm	1.8	1.8	nm	0.8	nm		1.00		0.42	

Additional material. Numerous specimens were extracted from the sediment. Nevertheless, this species has a quite fragile shell and it is difficult to obtain perfectly preserved material. Eighty-nine articulated partly preserved shells, 54 ventral and 148 dorsal valves (with broken spicular canopies) were observed.

Description. External characters. The shell is rather small, rarely exceeding 2 mm in length (Table 2), strong-

ly ventribiconvex, often longer than wide (Pl. 4, Fig. 1a) but subcircular specimens were also found (Pl. 4, Fig. 2a). The endopunctae are large. The anterior commissure is rectimarginate (Pl. 4, Fig. 1c) and the lateral commissure is straight (Pl. 4, Fig. 1b). The hinge line is straight.

The beak is medium sized. The interarea is transversely striated and a convex rugideltidium is developed. In juvenile specimens, the beak is weakly developed but the rugideltidium is already clearly visible (Text-Fig. 4.1a–d). The ventral valve is cemented by its posterior part (Pl. 4, Fig. 1b). Irregular growth lines are visible on the ventral valve surface (Pl. 4, Fig. 1b–c).

The dorsal valve is lid-like, weakly convex and has a subcircular or ovate outline. Growth lines are visible on its external surface. The highest part of the dorsal valve is the protegulum situated in the posterior part of the valve. It is visible better on juvenile specimens. It is more or less ovate and its surface is granular (Text-Fig. 4.1d).

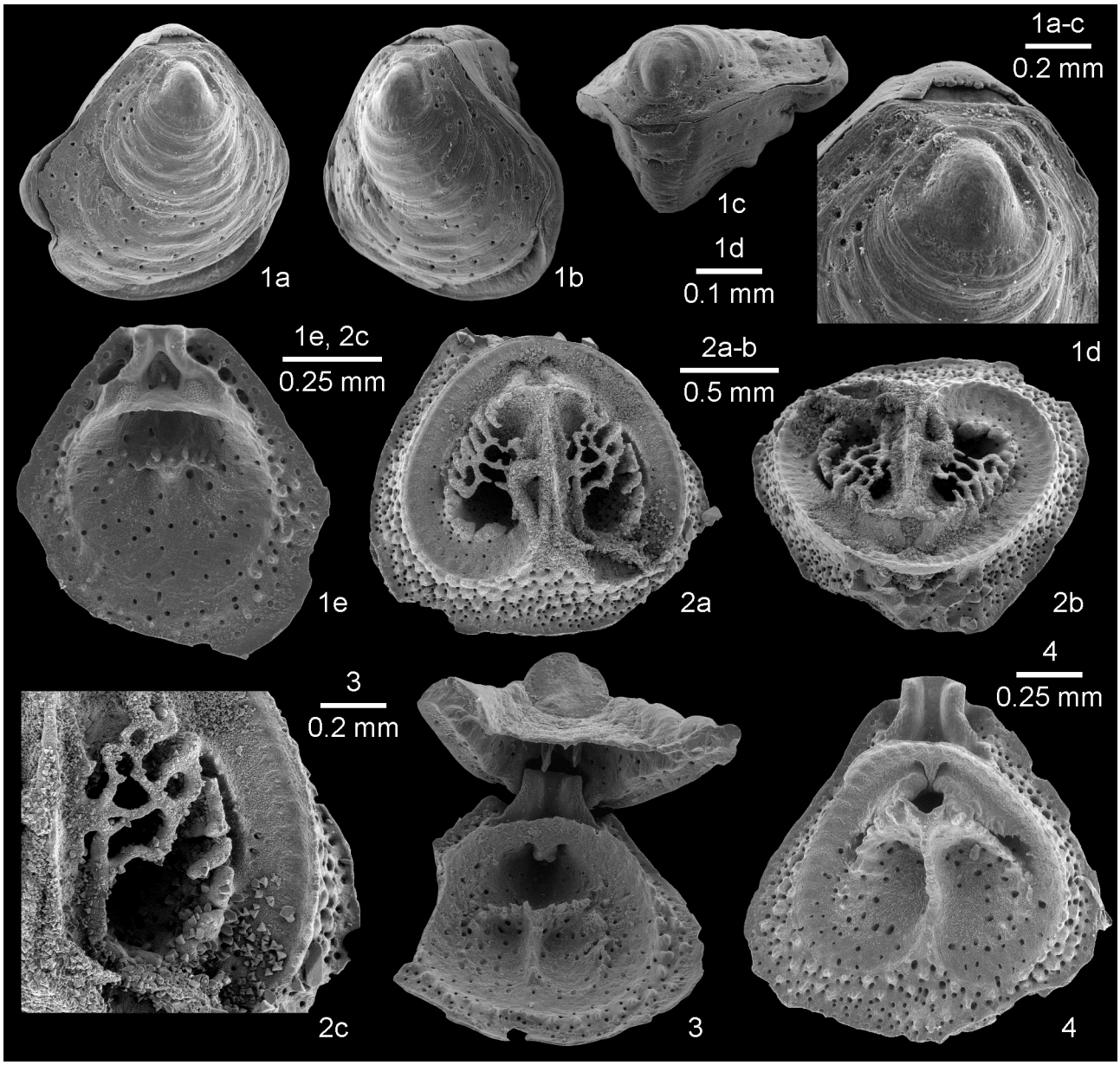

TEXT-FIGURE 4. *Minutella* cf. *minuta* (Cooper, 1981), "La Passe bateau" off the south-west coast of Mayotte Island. (1a–e) MNHN-IB-2017-173. a–d. Juvenile articulated specimen in dorsal, oblique lateral, posterior oblique views, and close-up of the posterior part of the shell (the protegulum is clearly limited by a step-like growth line and its surface is slightly granular; the rugideltidium is already well developed whereas the interarea remains reduced). e. Dorsal valve interior in plan view (early juvenile stage in the ontogeny of the dorsal valve). (2a–c) MNHN-IB-2017-174: dorsal valve interior with well-preserved spicular canopies in plan and oblique posterior views, and close-up of the spicular canopy. (3) MNHN-IB-2017-175: articulated specimen (young stage of growth). (4) MNHN-IB-2017-176: dorsal valve interior of a young specimen in plan view.

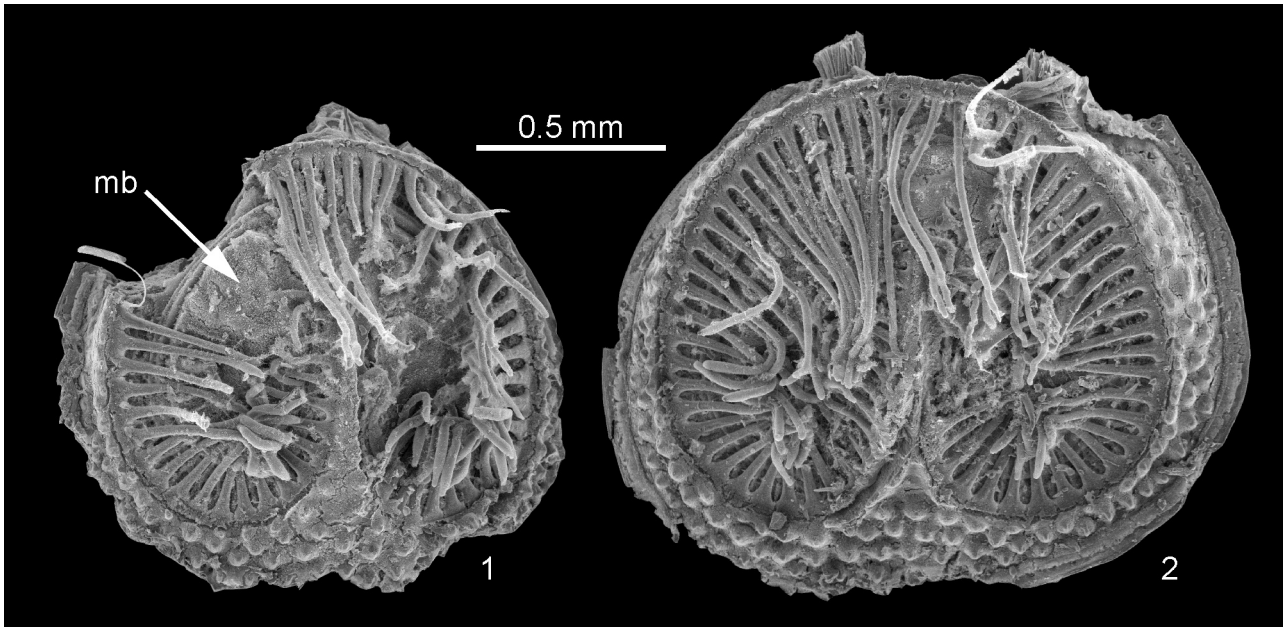

TEXT-FIGURE 5. *Minutella* cf. *minuta* (Cooper, 1981). Isolated dorsal valves of living specimens preserved in ethanol and critical point dried for SEM observation. The cardinal process has been broken when opening the shells. (1) MNHN-IB-2017-177: small adult specimen with the left side of the lophophore missing, allowing a view of the brachial cavity covered with a membrane (mb). (2) MNHN-IB-2017-178: Larger specimen. Both have a schizolophous lophophore.

Internal characters. In the ventral valve, a smooth-floored peripheral groove goes around the internal side of the commissures of the valve (Pl. 4, Fig. 3f). On the internal side of this groove a weakly tuberculate surface is developed. The ventral valve floor is strongly endopunctate with very large endopunctae and several tubercles are disseminated. In the posterior part, the tubercles are stronger and more numerous.

The hemispondylium is made of two quite wide subparallel prongs that are fused with the posterior part of the valve floor (Pl. 4, Fig. 3f). The teeth are short robust and covered with secondary shell material.

In the dorsal valve the structures developed rise toward the posterior part of the shell (Pl. 4, Fig. 3c). An extremely narrow, smooth flange is observed outside the peribrachial ridge (Pl. 4, Fig. 3a). The peribrachial ridge is ornamented with regularly placed tubercles that are better developed in the anterior part of the valve (Pl. 4, Fig. 3b, Text-Fig. 4.2a). The top of these tubercles shows a relief formed by two subparallel short ridges (Pl. 4, Fig. 3c).

A straight, very narrow median septum is developed. It flares widely in its anterior part. The ventral side of this septum is strongly concave, developing a groove toward its posterior part in well-preserved specimens (Pl. 4, Fig. 3b). The ventral edges of the septum are relatively regular and slightly spinous (Pl. 4, Fig. 3a). The lateral flanks of the septum constitute the inner walls of the brachial cavities and have a smooth surface (Pl. 4, Fig. 3a–c, Text-Fig. 4.2a–b).

The brachial cavities, or brood pouches, are deep and covered by spicular canopies, especially over the middle part of the cavities, to protect embryos. The spicules are irregular, very fragile and they form a network whose meshes vary in size and shape. Despite a first impression (Text-Fig. 4.2a), there is no precise symmetry between the canopy structures because the meshes are rather variable. The marsupial orifices are quite large.

The brachial bridge and the inner side of the peribrachial ridge have the same height and together form an ovoid structure with a smooth internal surface only marked by the regular lophophore muscle scars (Pl. 4, Fig. 3b, Text-Fig. 4.2a). The space between the peribrachial ridge and the external part of the brachial cavities, i.e. the lophophore groove, is heavily endopunctate especially in the anterior portion of the groove (Pl. 4, Fig. 3b–c, Text-Fig. 4.2a). The ventral edge of the brachial bridge is finely denticulate.

The posterior pointed tip of the dorsal septum is fused with the intrabrachial ridge. Two very tiny holes are perceptible on either side of the tip of the septum (Text-Fig. 4.2a). The visceral gap is rather small and has a regular ovate to diamond-shaped outline (Pl. 4, Fig. 3d, Text-Fig. 2b). A strong calcitic pole is present in the middle of this visceral gap. It is rather thick but short as it is not fused with the dorsal valve floor. There is a posterior excrescence on this calcitic pole but it is not very well developed (Pl. 4, Fig. 3d).

Posterior outgrowths protruding from the posterior side of the intrabrachial ridge extend towards the posterior part of the valve, partly filling the spaces on either side of the calcitic pole (Pl. 4, Fig. 3d, Text-Fig. 4.2b, 4).

The cardinal process is short, weakly curved and it is relatively narrow but very thick. Its anterior lateral sides are clearly pinched. The outer lateral lobes building the inner socket ridges are extremely thickened. This thickness appears very early in ontogeny as shown in Text-Fig. 4.3–4. Secondary shell material is deposited on these lateral lobes. The median lobe is moderately developed.

Lateral adductor muscle scars are clearly visible on either side of the visceral gap and have an ovate to kidney-shaped outline (Pl. 4, Fig. 3d).

The lophophore is schizolophous with around 80–85 tentacles at the adult stage of growth. All the tentacles are of the same length and thickness (Text-Fig. 5).

Remarks. The Indo-Pacific populations of *Minutella minuta* show certain morphological differences and these have already been discussed in Simon & Hoffmann (2013, pp. 411–412). No new species can be erected for now and further collections of new material are needed for molecular phylogenetic analyses. The problems are multiple: sufficient quantities of well-preserved material from all Indo-Pacific stations are, as yet, unavailable; perfectly fresh specimens are difficult to preserve in ethanol (thecideides have no foramen and when the living specimens are directly placed in ethanol their tightly closed shells do not allow the correct preservation of the soft parts); the stability of a particular character in a population must be evaluated by a large number of measurements allowing statistical analyses to confirm the taxonomical validity of accurate morphological characters.

Ontogeny of the shell. The complete sequence of the ontogeny of the shell in *Minutella* has been drawn in Simon & Hoffmann (2013, p. 410, pl. 2). Several sequences of this growth process have been illustrated in this paper (Text-Fig. 4.1e, 3–4). Compared with the previous study, the stages of growth are absolutely similar and no precise difference can be pointed out in the material collected from Mayotte.

FAMILY THECIDEIDAE GRAY, 1840

SUBFAMILY LACAZELLINAE BACKHAUS, 1959

Genus *Ospreyella* Lüter & Wörheide (in Lüter *et al.* 2003)

Type species. *Ospreyella depressa* Lüter (in Lüter *et al*. 2003), 2003 by original designation.

Emended diagnosis. See Simon & Hoffmann (2013, p. 412).

Ospreyella mayottensis Simon, Hiller, Logan & Mottequin, sp. nov.

Table 3; Text-Figs. 2, 6–7; Pl. 5, Figs. 1–2; Pl. 6, Figs. 1–8; Pl. 7, Figs. 1–6

? 1987 *Lacazella mauritiana* Dall, 1920: Zezina, p. 56, tab. 1.

Holotype. MNHN-IB-2017-179 (Text-Fig. 2; Pl. 5, Fig. 1), a fully female adult articulated specimen, which has been opened for the study of the brachidium.

Paratypes. MNHN-IB-2017-181 (Pl. 6, Fig. 1), MNHN-IB-2017-180 (Pl. 5, Fig. 2), MNHN-IB-2017-182 (Pl. 6, Fig. 2), and MNHN-IB-2017-183 (Pl. 6, Fig. 3), articulated specimens. MNHN-IB-2017-184 (Pl. 6, Fig. 4), dorsal valve of opened male specimen. MNHN-IB-2017-191 (pl. 7, fig. 3), MNHN-IB-2017-192 (Pl. 7, Fig. 4), MNHN-IB-2017-193 (Pl. 7, Fig. 5), and MNHN-IB-2017-194 (Pl. 7, Fig. 6), disarticulated or opened specimens used for ontogenetic study. MNHN-IB-2017-185 (pl. 6, Fig. 5), MNHN-IB-2017-187 (Pl. 6, Fig. 7), MNHN-IB-2017-188 (Pl. 6, Fig. 8), MNHN-IB-2017-186 (Pl. 6, Fig. 6), MNHN-IB-2017-190 (Pl. 7, Fig. 2), and MNHN-IB-2017-189 (Pl. 7, Fig. 1), opened specimens used for detailed views of specific parts of the shell. MNHN-IB-2017-196 (Text-Fig. 6.2) and MNHN-IB-2017-195 (Text-Fig. 6.1), specimens used for critical point analyses and study of the lophophore. Morphometric measurements of holotype and paratypes are presented in Table 3.

Etymology. The name of the species is the Latin translation of the Island of Mayotte.

Type locality. Department of Mayotte (France). Submarine cave at 23 m depth situated at La Passe bateau

off the south-west coast of the Island of Mayotte in the second coral reef barrier (Latitude: -12.9776, Longitude +44.9827).

Additional material. Material collected from the dried sieved sediment: 55 articulated specimens, 264 isolated dorsal and 40 isolated ventral valves. Material collected from samples of the walls of the cave and preserved in ethanol for study of the lophophore and future DNA studies: ten specimens.

Diagnosis. Medium-sized thecideide brachiopod (adult shell length around 3–5 mm). Female shells are as large as male shells and with similar complete ontogenetic development (gonochoristic species). Shell whitish, ventribiconvex, rectimarginate anteriorly.

Ventral valve with well-developed, triangular, convex rugideltidium, anterior part with numerous irregular cavities. Faint anterior sulcus present in some specimens, absent in others. Median ridge in the ventral valve present. Ventral valve floor with two types of spines. Hemispondylium formed by two inwardly concave, pointed, lateral prongs and a prominent median myophragm; no supporting structure of the hemispondylium is observed.

Dorsal valve with narrow and straight median ramus with subparallel frilled margins and concave ventral surface; ramuli much wider than median ramus, strongly concave with weakly frilled margins. Anterior median depression clearly developed and moderately wide. Anterior margin and peripheral ridge slightly tuberculated. Minor interbrachial lobes asymmetrical (one lobe always longer than the other one), weakly inwardly concave to straight, never furcated. Major intrabrachial lobes relatively regular, smooth with finely denticulate margins. Lophophore ptycholophous.

Diagnose. Brachiopode thécidéide de taille moyenne (les adultes ont une longueur de 3–5 mm). Les coquilles de spécimens femelles ou mâles ont une taille identique et un développement ontogénétique similaire. La coquille est blanchâtre, ventri-biconvexe avec une commissure rectimarginée.

La valve ventrale a une interarea triangulaire très développée avec un rugideltidium convexe dont la partie antérieure laisse apparaître de nombreuses cavités irrégulières. Un faible sulcus antérieur est parfois présent, parfois non. Le fond de la valve ventrale possède une crête médiane. Deux structures épineuses différentes se rencontrent sur le fond de la valve ventrale. L'hémispondylium est constitué de deux lames, concaves intérieurement dont l'extrémité est pointue et qui sont réunies par un solide myophragme médian ; l'hémispondylium est dépourvu de structures de support.

La valve dorsale a un ramus médian étroit, long nettement concave ventralement, avec des marges subparallèles épineuses. Les ramuli sont nettement plus larges que le ramus médian et ont marges faiblement épineuses. La dépression antérieure est présente et assez large. La bordure antérieure de la crête périphérique est légèrement tuberculée. Les lobes interbrachiaux mineurs sont asymétriques (un lobe toujours plus long que l'autre), plutôt tout droit ou très faiblement concave intérieurement et ne sont jamais divisés. Les lobes intrabrachiaux majeurs sont très réguliers, subcirculaires, lisses avec des marges très finement denticulées. Le lophophore est ptycholophe.

Description. External characters. The shell is relatively large for the genus (Table 3), reaching a width of about 5 mm (Table 3) and with a variable outline depending on the substrate to which the shell is fixed. It can have a drop-like aspect (Pl. 5, Fig. 2a; Pl. 6, Fig. 1a) but often it has an apple-shaped outline (Pl. 5, Fig. 1a; Pl. 6, Fig. 2). The maximum width (W) is at the mid-dorsal valve. The value of the length to width (L/W) ratio is constant and the shell keeps its outline unchanged during growth (Text-Fig. 7). The whitish shell is slightly longer than wide and is mainly cemented to the substrate by the posterior part of the ventral valve. Due to this type of attachment, the ventral part of the shell is often distorted (Pl. 5, Fig. 1d; Pl. 6, Fig. 1b, 1d). Rarely, the fixation of the shell occurs on its lateral part (Pl. 6, Fig. 2), a situation illustrating the strong influence of the substrate on the external shape of the shell.

The shell is strongly ventribiconvex (Pl. 5, Fig. 1b; Pl. 6, Fig. 1b), the dorsal valve being relatively flat, lid-like, except for its median part, which is slightly convex. During growth, the thickness of the shell increases relatively to its width, but the value of the thickness to width ratio (T/W) is not significantly modified (Text-Fig. 7). In dorsal view, the shell is sometimes cordiform as its anterior commissure is emarginate. In this case, a shallow median sulcus can develop at the anterior margin of the ventral valve (Pl. 5, Fig. 1a, 1c; Pl. 6, Fig. 1a, 1c) but this character is frequently absent. In lateral view, the entire shell is lifted from the substrate anteriorly (Pl. 5, Fig. 1b; Pl. 6, Fig. 1b), its anterior part tending to be in a more elevated position than the posterior one. Such a geniculation of the ventral valve is common in thecideide brachiopods as illustrated by Pajaud (1970, p. 219, fig. 130A). The anterior commissure is rectimarginate in anterior view (Pl. 5, Fig. 1c; Pl. 6, Fig. 1c). The lateral commissure is variable but generally concave dorsally.

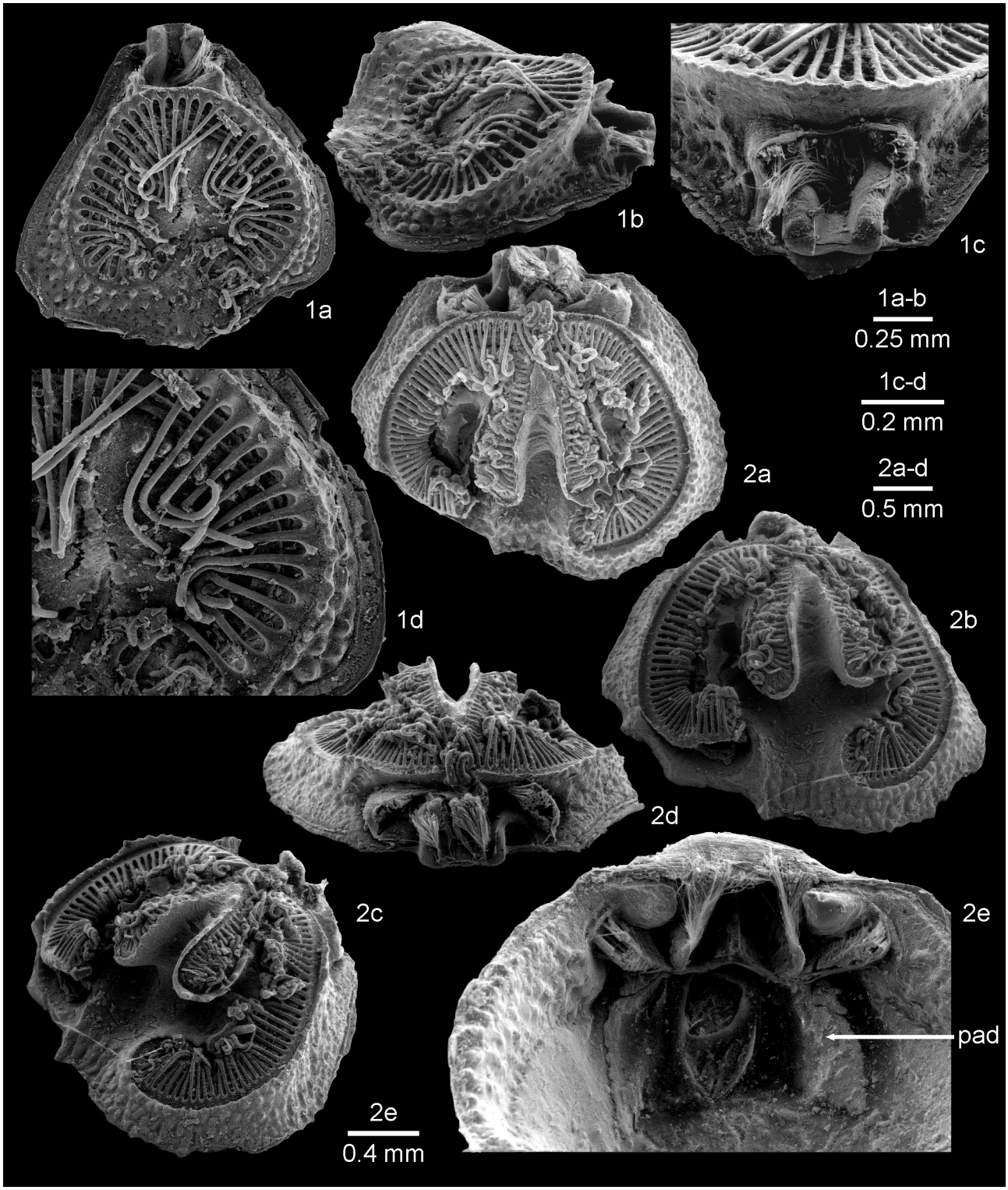

TEXT-FIGURE 6. Illustration of the lophophore in juvenile and adult specimens of *Ospreyella mayottensis* **sp. nov.** from "La Passe bateau" off the south-west coast of Mayotte Island. (1a–d) MNHN-IB-2017-195 (paratype): a juvenile dorsal valve interior in plan and oblique lateral views (schizolophous lophophore including between 45–48 tentacles), close-up of the posterior part of the valve with the muscles, and detailed view of the right side of the lophophore. (2a–e) MNHN-IB-2017-196 (paratype): an adult disarticulated specimen. a–d. Dorsal valve interior showing the ptycholophous lophophore (around 140 tentacles) in plan, oblique anterior and oblique anterolateral views. e. Ventral valve interior in oblique anterior view (critical point dried) showing the two pads covering the gonads (on the right side the pad is still placed correctly (pad) whereas on the left side, the pad has moved laterally).

TABLE 3. *Ospreyella mayottensis* **sp. nov.** Morphometric measurements were taken for the holotype, for the paratypes and for a large number of articulated individuals collected from the sieved sediment collected in the submarine cave in Mayotte at 23 m depth. Male and female specimens are of the same size range. Abbreviations: N, number of specimens measured; MIN, minimum; MAX, maximum; L, length, W, width; LD, length of dorsal valve; Lint, length of the interarea; Wint, width of the hinge or interarea; T, thickness; nm, value not measured.

Illustrated specimens	**L**	**W**	**LDV**	**Lint**	**Wint**	**T (max)**	**L/W**	**LDV/W**	**Lint/W**	**Wint/W**	**T/W**
	mm	**mm**	**mm**	**mm**	**mm**	**mm**					
Holotype MNHN-IB-179	3.5	3.6	2.9	0.5	2.1	nm	0.96	0.81	0.15	0.58	
Paratype MNHN-IB-180	3.6	3.6	2.5	1.1	1.9	2.6	1.00	0.69	0.31	0.51	0.72
Paratype MNHN-IB-181	4.2	3.8	2.9	1.1	2.1	2.3	1.11	0.77	0.28	0.56	0.61
Paratype MNHN-IB-182	4.3	4.0	2.9	1.4	2.5	2.7	1.09	0.73	0.35	0.63	0.67
Paratype MNHN-IB-183	nm	5.1	nm	nm	nm	nm					
Paratype MNHN-IB-184	nm	3.7	3.0	nm	2.0	nm		0.83		0.53	
Paratype MNHN-IB-185	3.9	3.7	2.8	1.1	2.1	nm	1.05	0.75	0.29	0.57	
Paratype MNHN-IB-192	nm	1.4	1.3	nm	0.5	nm		0.94		0.35	
Paratype MNHN-IB-193	3.4	3.2	2.7	0.6	1.1	nm	1.06	0.85	0.21	0.34	
Paratype MNHN-IB-194	nm	3.6	2.6	nm	1.9	nm		0.72		0.53	
Paratype MNHN-IB-195	nm	1.4	1.4	nm	0.5	nm		0.99		0.34	
Paratype MNHN-IB-196	nm	3.2	2.6	nm	1.8	nm		0.81		0.56	
Total measurements											
N	66	111	110	66	74	37	66	110	66	74	37
Mean value	3.9	3.4	2.6	1.1	1.9	2.0	1.07	0.79	0.29	0.54	0.54
MIN	0.8	0.9	0.6	0.1	0.3	0.3	0.70	0.56	0.03	0.30	0.15
MAX	5.9	5.1	3.8	2.5	3.2	3.2	1.33	1.10	0.55	0.72	0.83
Standard deviation	1.0247	0.9042	0.6328	0.5551	0.7244	0.6495	0.1330	0.0991	0.1199	0.1018	0.1329
Standard error (±)	0.1261	0.0858	0.0603	0.0683	0.0842	0.1068	0.0164	0.0094	0.0148	0.0118	0.0218

The ventral valve has a relatively long and strongly produced beak with a flat triangular interarea ornamented with numerous fine regular growth lines, parallel to the hinge line. A raised triangular, transversely convex rugideltidium is developed (Pl. 5, Figs. 1a, 1d, 2a–e; Pl. 6, Figs. 1a, 1d, 2, 5a, 7). The rugideltidium is quite long and can represent up to 30 % of total shell length. The dorsal surface of the rugideltidium is flatly-convex, irregular and growth lines are not very distinct (Pl. 6, Fig. 1a). The interarea and the convex rugideltidium are usually straight but often they may be strongly curved to the right or to the left. The anterior part of the rugideltidium is normally smooth but, if this surface is eroded, the internal structure of the rugideltidium becomes visible and is made of numerous irregular cavities that are not endopunctae (Pl. 5, Fig. 2b; Pl. 6, Fig. 5c).

Subparallel undulating growth lines are visible on the external ventral shell surface and their thickness is variable (Pl. 6, Fig. 1c).

The lid-like dorsal valve is always wider than long, oval in shape and often with an emarginate anterior commissure (Pl. 5, Fig. 1a; Pl. 6, Figs. 1a, 2). On the dorsal valve surface, the growth lines are indistinct and irregular. The protegulum is prominent and has a granular surface (Pl. 5, Fig. 2b; Pl. 6, Fig. 8).

The hinge line is straight and always narrower than the maximum width of the valve (Table 3). The length of the hinge line increases during growth as indicated by the values of the width of the hinge to the width of the shell (WH/W) ratio (Table 3, Text-Fig. 7).

Most of the morphological characters show a linear variation when compared to value of the width of the shell (Text-Fig. 7). However, the best fitting relation between the length of the interarea and the width of the shell is an exponential variation (Text-Fig. 7). This explains the big difference between the beak length in juveniles and in adult specimens (Table 3).

Internal shell characters. The ventral valve has a drop-like, slightly bilobed and cordiform outline due to its emarginate anterior commissure (Pl. 5, Figs. 1l, 2c; Pl. 6, Fig. 5a). All around the commissure is a smooth peripheral flange, which seals the shell when the valves are closed. The commissure is limited internally by a peripheral rim with a smooth external side and a row of more or less regular, strong tubercles on the internal side (Pl. 5, Fig. 2c, 2e; Pl. 6, Figs. 5a).

A wide median ridge is visible in the middle of the ventral valve floor. This median ridge separates the two deep gonad pits placed in the posterior part of the valve (Pl. 5, Fig. 2c, 2e; Pl. 6, Fig. 5a). The valve floor shows endopunctae and is roughly granulated. At high magnification the surface appears to be ornamented with small spinous asperities (Pl. 7, Fig. 1a). At higher magnification, two kinds of spines are discovered: there are small narrow cylindrical spines (less numerous) and there are wider conical structures that are more numerous (Pl. 7, Fig. 1a–b). The role of such very peculiar ornamentation remains unknown.

The strong cyrtomatodont teeth are short, relatively thick, and reinforced with secondary shell material (Pl. 6, Fig. 5b). The hemispondylium consists of two pointed lateral prongs and a prominent median lamellar myophragm (Pl. 5, Figs. 1l, 2e: Pl. 6, Fig. 5b). A septum supporting the hemispondylium is not observed in adult or young specimens.

In specimens collected alive and treated using the critical point method, two calcitic oval pads covering the gonads are visible in the posterior part of the ventral valve floor (Text-Fig. 6.2e). In this illustration, the right plate is still in its correct position whereas the left one has moved laterally. The external edge of this calcitic plate is denticulate. In female specimens a median brood pouch containing the larvae is situated between the gonad pads.

The dorsal valve in ventral view is widely oval, usually with an emarginate anterior commissure (Pl. 5, Fig. 1e) but sometimes the valve is not emarginate (Pl. 6, Fig. 4a). In completely preserved specimens a narrow smooth, flat flange is present along the commissure (Pl. 6, Fig. 4a–d). The peribrachial ridge is covered with numerous tubercles that can have a highly variable outline. They can be subspherical with a moderate size and a cup-like aspect (Pl. 5, Fig. 1i) or strong irregular tubercles (Pl. 6, Fig. 4b–c) and sometimes showing a mixed ornamentation (Text-Fig. 6.2a–b).

The dental sockets are strong, formed by curved inner socket ridges and totally flat, depressed, outer socket ridges (Pl. 5, Fig. 1e, j–k; Pl. 6, Fig. 4d). The trilobed cardinal process (Pl. 5, Fig. 1k; Pl. 6, Fig. 4d) has a wide smooth ventral surface and is curved dorsally. Secondary shell material thickens the lateral parts (Pl. 5, Fig. 1k; Pl. 6, Fig. 4d). The development of the median lobe is most prominent in its posterior part.

Wide drop-like lateral adductor muscle scars are clearly developed on either side of the cardinal process (Pl. 5, Fig. 1k; Pl. 6, Fig. 4d). Between the cardinal process and the brachial bridge, a heart-shaped visceral foramen (Pl. 5, Fig. 1k; Pl. 6, Fig. 4d), free of a calcitic pole, is apparent. The diductor muscle scars are sometimes visible on the posterior margin of the cardinal process (Pl. 6, Fig. 4d) but they are weakly defined.

The shell structures developed in the dorsal valve are slightly raised towards the posterior part of the valve (Pl. 7, Fig. 4c). A thin and relatively narrow brachial bridge (Pl. 5, Fig. 1k) is built by the fusion of the posterior parts of the peribrachial ridge margin (similar to a fusion of crural processes as proposed by Logan (2008, p. 411)). This brachial bridge is thin and remains complete in male specimens (Pl. 6, Fig. 4a, 4d) but is interrupted by a marsupial notch in female specimens (Pl. 5, Fig. 1e, 1g, 1i-k). The marsupial notch is a small subcircular hole open on the ventral side of the brachial bridge. The posterior face of the marsupial notch exhibits a small platform with a small convex median ridge (Pl. 5, Fig. 1g; Pl. 7, Fig. 2a–b) and a short posterior point. The inner surface of the marsupial notch exhibits the muscle scars of the pair of specialized tentacles (Pl. 5, Fig. 1g) that are related to the development of the embryos in the brood pouch (Text-Fig. 6.2d).

The lophophore is attached to the lophophore groove that follows the internal side of the peribrachial ridge, the external sides of the ramuli and the lateral sides of the median ramus (Pl. 5, Fig. 1e; Pl. 6, Fig. 4a) and the lophophore muscle scars are clearly defined by numerous parallel imprints.

The margins of the intrabrachial ridges exhibit short spines (Pl. 5, Fig. 1e–f) that can be very weakly developed in some specimens (Pl. 6, Fig. 4a–b).

In their posterior part, the margins of the major intrabrachial lobes are connected by means of the jugum (Pl. 5, Fig. 1f; Pl. 6, Fig. 4a). The major intrabrachial lobes are widely developed in this species and have a very regular subcircular outline. Their ventral surfaces are smooth but their external margins are finely and regularly denticulate.

Two subparallel minor interbrachial lobes extend anteriorly from either side of the jugum. These are relatively long and thick with rather sharp edges; their ventral surfaces are granular (Pl. 5, Fig. 1f). They are never observed to be divided or furcated in any of our specimens. The development of the minor interbrachial lobes is asymmetrical (Pl. 5, Fig. 1f; Pl. 6, Fig. 4a), with the longer lobe indifferently the right or the left one.

The pointed median ramus has a strongly concave upper surface, a relatively long and narrow triangular outline with frilled lateral margins and is connected posteriorly by the small jugum (Pl. 5, Fig. 1f) to the intrabrachial ridge. The median ramus remains strongly concave throughout ontogeny and it is never filled by secondary shell material. The length of the median ramus is variable; it originates from the middle or sometimes a little more anterior part of the valve. The median ramus is attached to the valve floor by a triangular base developed in the middle of the anterior part of the valve (Pl. 6, Fig. 4b).

Two strong lateral ramuli are well-developed. The ramuli are wider than the median ramus and their upper surfaces are deeply concave, a morphology maintained throughout ontogeny. They are never thickened by deposition of secondary shell material. The lateral margins of the ramuli are ornamented with several irregular spines on both sides.

The median anterior depression is relatively narrow, its anterior margin being limited by the tuberculated peripheral rim. The ascending apparatus and the descending apparatus are developed symmetrically (Pl. 5, Fig. 1e; Pl. 6, Fig. 4a).

The adult lophophore is ptycholophous with approximately 160 tentacles observed in an adult female specimen (Text-Fig. 6.2b). At the trocholophous stage, the lophophore possesses 27 tentacles (Simon & Hoffmann 2013, pl. 4, fig. 1) but this number increases rapidly and 46–50 tentacles are observed in a young schizolophous developmental stage (Text-Fig. 6.1a). In male specimens, the lophophore is developed regularly whereas in females, the lophophore is interrupted posteriorly, allowing the development of a pair of specialized median tentacles (Text-Fig. 6.2a, c). A complete ontogeny of the lophophore is not available as trocholophe and other intermediate stages of growth were not found in our limited material preserved in ethanol.

Comparison with other species of *Ospreyella*. *Ospreyella mayottensis* **sp. nov.** is directly distinguished from *O. depressa* Lüter (in Lüter *et al.* 2003) and from *O. maldiviana* Logan, 2005 by its minor interbrachial lobes which are never furcated as they are in the two other species.

The external aspect of *O. palauensis* Logan, 2008 is more subcircular. *O. palauensis* is distinct from *O. mayottensis* **sp. nov.** by its minor interbrachial lobes which are stronger and straighter in the latter. In *O. palauensis* they have also a tendency to furcation. The median ramus in *O. mayottensis* **sp. nov.** is straighter, regularly triangular and longer than in *O. palauensis* where it is shorter and with a much more variable outline. Moreover, the median ramus can be divided in *O. palauensis* when furcation of the minor interbrachial lobes occurs.

The Australian *Ospreyella* sp. from Lizard Island is known from very few specimens (Hoffmann *et al*., 2009). At first glance the major intrabrachial lobes in *Ospreyella* sp. have more strongly spinous external margins and the

median ramus is rather shorter than in *O. mayottensis* **sp. nov.** The ramuli of *Ospreyella* sp. are poorly developed but the specimens illustrated by Hoffmann *et al.* (2009) are maybe still at a juvenile stage of growth and do not allow for an accurate comparison.

O. mutiara Simon & Hoffmann, 2013 has a more subrectangular outline for its dorsal valve. The major intrabrachial lobes are relatively narrower. The median ramus and the ramuli in *O. mutiara* are thickened by accretion of secondary shell material through ontogeny. The median ramus and the ramuli have a similar width and the margins of the ramuli are strongly and regularly spinous (Simon & Hoffmann 2013, pl. 5). As *O. mutiara* is hermaphroditic with a protandry, males are much smaller than females. In *O. mayottensis* **sp. nov.** the dorsal valve is more subcircular. The major intrabrachial lobes are relatively larger and wider. The median ramus and the ramuli are very different, the median ramus being narrow, whereas the ramuli are very wide. Both are markedly concave and not thickened through ontogeny. *O. mayottensis* **sp. nov.** is gonochoristic and both shells of male and female are of the same size.

Ospreyella sp. collected from Europa Island (Mozambique Channel, off south-west Madagascar) displays some similarities with *O. mayottensis* **sp. nov.** (Simon & Hoffmann 2013, pl. 8) but the external aspect of *O.* sp. is more widely oval with a much shorter interarea (Simon & Hoffmann 2013, pl. 8, figs. 1a–b, 2). The median ramus is much more variable in outline in *Ospreyella* sp. with more asymmetrical structures of the *apparatus descendens* and *ascendens*. A tendency to furcation of the minor interbrachial lobes is visible in *Ospreyella* sp. from Europa Island (see Simon & Hoffmann, 2013: plate 8, fig. 5), a character that is never observed in *O. mayottensis* **sp. nov.** The latter is also the simplest and the most subsymmetrical species with its regular subcircular major intrabrachial lobe.

The lacazelline material from Secteur de Poindimié (stn. 830) in New Caledonia, collected at 105–110 m depth has been wrongly assigned by Bitner (2010, p. 654, fig. 6) to the genus *Lacazella* Munier-Chalmas, 1880. This genus has a Mediterranean–Caribbean–Atlantic distribution and it is not present in the Pacific (Simon & Hoffmann 2013, p. 430). This has been shown by both morphological and molecular approaches. This material should be attributed to an unidentified *Ospreyella* species. The wide anterior depression and the median ramus emerging directly from the middle of the valve floor and not supported by a septum in these specimens confirm this proposition. It is difficult to compare accurately *O. mayottensis* **sp. nov.** with this New Caledonian material as its preservation is not excellent. If a sexual dimorphism exists in this species, it cannot be pointed out, as all the brachial bridges are broken. However, the median ramus seems to be sometimes as wide as the ramuli (Bitner 2010, fig. 6D–E) or sometimes much more reduced (Bitner 2010, fig. 6H). Such a wide variation is not visible in *O. mayottensis* **sp. nov.** The minor interbrachial lobes are also shorter in the New Caledonian material.

Shell ontogeny. The shell ontogeny of *O. mayottensis* **sp. nov.** follows a lacazelline model. It is very similar to the ontogeny already studied for other species, such as *O. palauensis* Logan, 2008 and *O. mutiara* Simon & Hoffmann, 2013. Water movements in the submarine cave weaken the juvenile shells and it has been difficult to find perfectly intact juveniles. However, the main steps of the ontogeny are illustrated in Pl. 7, Figs. 3-6.

A V-shaped structure consisting of two divergent spikes appears in the middle of the valve floor. The two spikes are separated from each other at their bases. The lateral parts of the peribrachial ridge start to develop as small tubercles (Pl. 7, Fig. 3). The brachial bridge is not completely built.

The median ramus emerges in front of the divergent spikes and it develops anteriorly. The two spikes fuse together at their base. The two divergent processes form the beginning of the major intrabrachial lobes. Initially, these grow posteriorly, then bend laterally and turn anteriorly forming the first stages of the *apparatus descendens* (Backhaus 1959). These early major brachial lobes appear as two ears with a quite irregular outline (Pl. 7, Fig. 4a–c). Later, the major intrabrachial lobes present an "M"-shaped structure with its extremities slightly widened, giving them a spoon-like aspect.

The peribrachial ridge becomes better developed with more numerous coalescent tubercles and a peripheral flange is clearly visible (Pl. 7, Fig. 4c). Normally, the brachial bridge should be fully developed but a well-preserved specimen has not been found.

The median ramus remains quite small and a submedian elongated shell structure, consisting of two faint ridges, emerges at the anterior base of the median ramus and reaches the anterior part of the valve (Pl. 7, Fig. 5b). The ridges limit the future development of the median depression. The median ramus, which appears as a pointed knob placed at the posterior part of the submedian ridges (Pl. 7, Fig. 5b–c), is related with the jugum, which is connected with the growing major intrabrachial lobes. These new structures are raised from the dorsal valve floor.

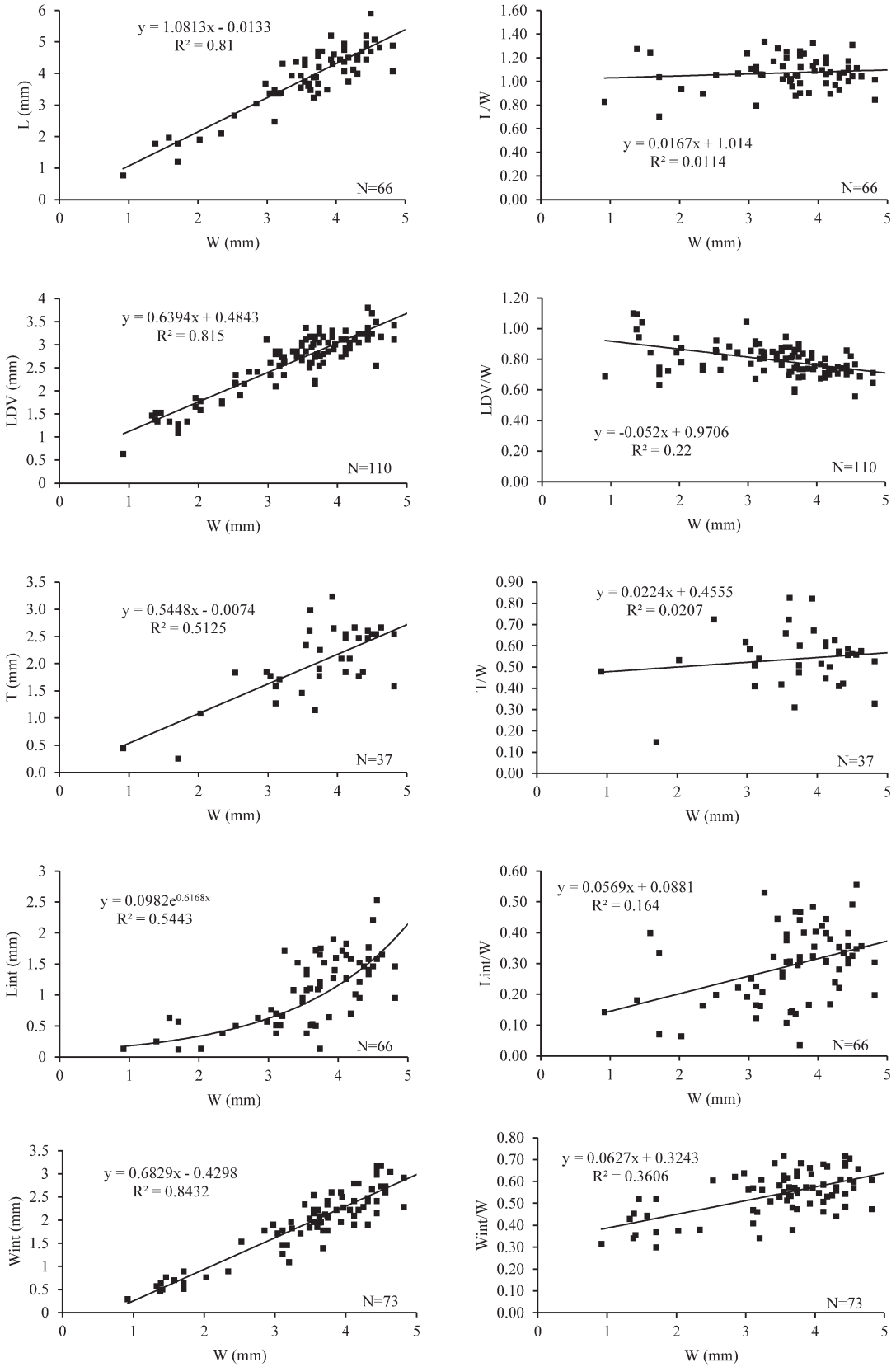

TEXT-FIGURE 7. Scatterplots of morphometric measurements of *Ospreyella mayottensis* **sp. nov.** Abbreviations: L, length; W, width; LDV, length of dorsal valve; T, thickness; Lint, length of the interarea, Wint: width of hinge line or interarea. Relationships between ratios L/W and width, LDV/W and width, T/W and width, Lint/W and width and Wint/W and width. Linear regression and regression coefficient (R^2) indicated except for the graph between Lint and width for which an exponential regression is fitting better. The regression coefficient (R^2) is indicated. N is the number of specimens measured.

The ramuli also develop at this stage of growth and they are already wider than the precursor of the median ramus (Pl. 7, Fig. 5b). The brachial bridge is clearly visible and no calcitic pole is produced as is the case in lacazelline thecideides. The tubercles defining the peribrachial ridge are more or less completely fused (Pl. 7, Fig. 5b–c).

The ventral valve shows all the adult characters as the hemispondylium and the rugideltidium are completely formed (Pl. 7, Fig. 5a).

Later, the major intrabrachial ridges reach nearly their adult subcircular outline with a smooth ventral concave surface and finely denticulate margins. The minor interbrachial lobes grow progressively (Pl. 7, Fig. 6a: the left minor interbrachial lobe has been broken). The anterior depression is achieved. The wide ramuli extend and they have frilled margins. The median ramus, remains narrow but it grows in length (Pl. 7, Fig. 6a–c).

The ventral valve floor becomes more spinous with the two types of spines: several narrow cylindrical spines and more numerous wide conical spines (Pl. 6, Fig. 6d).

Structure of the lophophore. After the earliest stage, which is a trocholophe type (Simon & Hoffmann 2013, pl. 4, fig. 1), the lophophore becomes schizolophous (Text-Fig. 6.1a–b, d). The number of tentacles increases rapidly as it reaches around 45–48 tentacles at this stage of growth.

At the adult growth stage, the lophophore becomes ptycholophous (Text-Fig. 6.2a–d). The number of tentacles is around 140. The filaments are not furcated and seem to have a smooth surface. The lophophore at this stage of growth is attached along the internal side of the peribrachial ridge and along the external sides of the median ramus. The internal parts of the median ramus and of the ramuli are free from the lophophore and are used to facilitate water circulation.

Discussion

The number of extant species of brachiopods is quite reduced in comparison with the huge representation of this phylum that was dominant in Palaeozoic seas. However, each new expedition in all seas of the world discovers new species obtained mainly by trawling or dredging methods. Scuba-diving also provides a lot of new species of brachiopods when cryptic environments, such as submarine caves, are prospected (Logan & Zibrowius 1994; Simon & Willems 1999; Simon *et al*. 2018b) and also shipwrecks (Simon 2010; Simon & Hoffmann 2013; Simon *et al.* 2016). Shipwrecks are, moreover, large enclosed spaces where small specimens of brachiopods can accumulate without significant alterations. Submarine caves are also an ideal natural cryptic environment for the development of brachiopods but the conditions for collecting them are more delicate.

Thecideide brachiopods are mostly shallow water species and they are often found as dominant species in such environments. This is again the case in this Mayotte submarine cave where *Thecidellina leipnitzae* **sp. nov.** is the dominant brachiopod followed by *Minutella* cf. *minuta* (Cooper, 1981) and by *Ospreyella mayottensis* **sp. nov.**

Although the Mozambique Channel is not frequently prospected by marine expeditions, numerous brachiopods have already been collected from this area but generally from rather deep waters (Bitner & Logan 2016). For this reason, thecideide brachiopods remain undescribed except for *Thecidellina europa* Logan *et al*., 2015.

The morphological characters of *T. europa*, which was discovered in the southern part of the Mozambique Channel, distinguish it from *T. leipnitzae* **sp. nov.** described in this paper. The uniform ventral valve floor and the broad dorsal septum grooved anteriorly with a prominent ridge at its posterior tip are characters of *T. europa* that are not seen in *T. leipnitzae* **sp. nov.** This species is apparently only known from the area of Mayotte Island, situated at the northern limit of the Mozambique Channel. The two islands are separated by 1,200 km. This configuration recalls the Caribbean distribution of the genus *Thecidellina* that is represented by the type species *T. barretti* (Davidson, 1864) and a second one, namely *T. bahamiensis* Lüter & Logan *in* Lüter *et al.*, 2008. *Thecidellina williamsi* Lüter & Logan *in* Lüter *et al.*, 2008 from Cabo Verde is a third species pertaining to this issue. All three were at first glance considered as populations of *T. barretti*. Nevertheless, accurate observations of their morphological characters led Lüter *et al*. (2008) to distinguish three species that are the result of allopatric speciation processes.

In the case of *T. europa* and *T. leipnitzae* **sp. nov.** allopatric speciation has also occurred and detailed observations of their morphological characters immediately separate both species. Molecular analysis of the material preserved in ethanol should provide a confirmation of this in the future. It is now obvious that the genus *Thecidellina* has a strong potential for allopatric speciation and this new case from Mayotte Island is a supplementary confirmation of a general population genetic behavior of this genus.

An interesting supplementary study would be an investigation of the thecideide brachiopod faunas from Juan de Nova Island, situated in the middle part of the Mozambique Channel, and from Bassas da India Island, which is quite close to Europa Island (110 km) (Text-Fig. 1). Similarities or differences between the faunal composition of these other islands and the faunal composition of Europa and Mayotte islands could yield a lot of useful information concerning allopatric speciation within the genus *Thecidellina* in this geographical area.

Ospreyella mayottensis **sp. nov.** is a new species added to the Indo-Pacific genus *Ospreyella* discovered in 2003. It is now clearly established by morphological and molecular results that the genus *Lacazella* is an Atlantic lacazelline (Simon & Hoffmann 2013). Since 2003, seven new *Ospreyella* species have been erected and several undescribed *Ospreyella* sp. and wrongly attributed *Lacazella* sp. suggest that the total number of species in this genus is significantly larger. The geographical distribution of the genus covers nearly all the Indo-Pacific as it is found from New Caledonia, Australia, Indonesia, the Palau Archipelago in the East and the Maldive Islands and the Mozambique Channel in the West. This genus seems to have also a strong aptitude for allopatric speciation. The distance between two different species can be quite short as is the case for *O. depressa* in the Osprey Reef and *O.* sp. in Lizard Island, Great Barrier Reef. Both locations are separated by only 160 km. On the contrary, *Ospreyella mutiara* from central Sulawesi and *O. palauensis* in Palau Archipelago are separated by 1,870 km. The genera *Ospreyella* and *Thecidellina* have a similar model of speciation. This indicates that continuous research of thecideide brachiopods in all the remaining areas of the world that are yet to be prospected could rapidly reveal an unsuspected wealth of new species.

Concerning *Minutella minuta*, its presence in all the Indo-Pacific stations investigated is a question in itself. The genus *Minutella* is present in Caribbean and in Indo-Pacific waters. There are clear differences between the Caribbean and the Indo-Pacific species (Simon & Hoffmann 2013) such as the width of the dorsal septum for instance, which is much wider in Caribbean species. In this restricted area two species have been found, namely *Minutella tristani* Hoffmann & Lüter, 2010 and *M. bruntoni* Hoffmann & Lüter, 2010. The genus seems to follow the same type of speciation as *Thecidellina*.

In the whole Indo-Pacific, the presence of a unique species, *M. minuta*, is astonishing, especially when considering the diversified radiation of the species of *Thecidellina* and *Ospreyella*. In actual fact, a lot of small differences between the morphological characters of the different Indo-Pacific "populations" have been described. For instance, the regular circular holes observed in the spicular canopies of *M. minuta* (Indonesian form) are never observed in the specimens from Samper Bank (Madagascar) and from Mayotte. Nonetheless, all the specimens of the Indonesian form are devoid of this character and there are exceptions with polygonal holes. It is like that with all the morphological distinctions described in the Indo-Pacific area. This does not mean that different species of *Minutella* could not be erected but the morphology gives no sufficiently conclusive arguments. So molecular analyses are needed and should be conducted on all the known "populations" to finally remove doubts that remain.

Acknowledgments

†Eric Simon passed away suddenly on 11 February 2018 after a career dedicated to the teaching of biochemistry and microbiology in higher education institutions until his retirement in 2013. In the meantime, he developed an acknowledged expertise in Cretaceous and Recent brachiopods. His scientific open-mindedness and his convivial attitude will be deeply missed.

We want to express our sincere thanks to C. Perron (Manager of the Marine Park of Mayotte) who authorized us to collect sediments in the submarine cave and who sustained us in our project to study local brachiopods. J. Cillis (RBINS Brussels, Belgium) is acknowledged for his help in using the SEM and for the excellent photographs.

The manuscript benefited from the thorough reviews of J. Robinson (Dunedin, New Zealand) and from an anonymous reviewer, and from the editorial help of Daphne Lee (Dunedin, New Zealand).

References

Backhaus, E. (1959) Monographie der cretacischen Thecideidae (Brach.). *Mitteilungen aus dem geologischen Staatinstitut Hamburg*, 28, 5–90.

Baker, P.G. (2006) Thecideoidea. *In*: Kaesler, R.L. (Ed.), *Treatise on Invertebrate Paleontology. Part H. Brachiopoda, 5. Re-*

vised. Geological Society of America, Boulder, Colorado and University of Kansas Press, Lawrence, Kansas, pp. 1948–1964.
Baker, P.G. & Carlson, S.J. (2010) The early ontogeny of Jurassic thecideoid brachiopods and its contribution to the understanding of thecideoid ancestry. *Palaeontology*, 53, 645–667.
http://doi.org/10.1111/j.1475-4983.2010.00941.x
Bitner, M.A. (2009) Recent Brachiopoda from the Norfolk Ridge, New Caledonia, with description of four new species. *Zootaxa*, 2235, 1–39.
Bitner, M.A. (2010) Biodiversity of shallow-water brachiopods from New Caledonia, SW Pacific, with description of a new species. *Scientia marina*, 74 (4), 643–657.
http://doi.org/10.3989/scimar.2010.74n4643
Bitner, M.A. & Logan, A. (2016) Recent Brachiopods from the Mozambique–Madagascar area, western Indian Ocean. *Zoosystema*, 38 (1), 5–41.
http://doi.org/10.5252/z2016n1a1
Cohen, B.L., Gawthrop, A. & Cavalier-Smith, T. (1988) Molecular phylogeny of brachiopods and phoronids based on nuclear-encoded small subunit ribosomal RNA gene sequences. *Philosophical Transactions of the Royal Society of London*, B 353, 2039–2061.
http://doi.org/10.1098/rstb.1998.0351
Cohen, B.L. & Gawthrop, A.B. (1996) Brachiopod molecular phylogeny. *In*: Copper, P. & Jin, J. (Eds.), *Proceedings of the Third International Brachiopod Congress, Sudbury/Ontario/Canada/2–5 September 1995*. A.A. Balkema, Rotterdam, Brookfield, pp. 73–80.
https://doi.org/10.1201/9781315138602-14
Cooper, G.A. (1954) Recent brachiopods. *In*: Bikini and nearby atolls, Marshall Islands. Part 2. Oceanography (biologic). *United States Geological Survey Professional Paper*, 260G, 315–318.
http://doi.org/10.3133/pp260g
Cooper, G.A. (1973) New Brachiopoda from the Indian Ocean. *Smithsonian Contributions to Paleobiology*, 6, 1–43.
http://doi.org/10.5479/si.00810266.16.1
Cooper, G.A. (1981) Brachiopoda from Southern Indian Ocean (recent). *Smithsonian Contributions to Paleobiology*, 43, 1–93.
http://doi.org/10.5479/si.00810266.43.1
Dall, W.H. (1920) Annotated list of the Recent Brachiopoda in the collection of the United States National Museum, with description of thirty-three new forms. *Proceedings of the United States National Museum*, 57 (2314), 261–377.
http://doi.org/10.5962/bhl.title.136940
Davidson, T. (1864) On the recent and Tertiary species of the genus *Thecidium*. *Geological Magazine*, 1, 12–22.
http://doi.org/10.1017/s0016756800469803
Duméril, A.M.C. (1805) *Zoologie analytique ou méthode naturelle de classification des animaux*. Allais, Paris, XXIV + 344 pp.
Elliott, G.F. (1953) The classification of the thecidean brachiopods. *The Annals and Magazine of Natural History*, Series 12, 6 (69), 693–701.
http://doi.org/10.1080/00222935308654471
Elliott, G.F. (1958) Classification of thecidean brachiopods. *Journal of Paleontology*, 32, 373.
Gray, J.E. (1840) *Synopsis of the Contents of the British Museum*. *42nd Edition. G. Woodfall, London*, 370 pp.
Hayasaka, L. (1938) A new Neotreme genus of Brachiopod from Japan. *The Venus*, 8, 9–13.
Hedley, C. (1899) The Mollusca of Funafuti. Part II. Pelecypoda and Brachiopoda. *Memoirs of the Australian Museum*, 3, 491–510.
http://doi.org/10.3853/j.0067-1967.3.1899.504
Hiller, N. (1986) The South African Museum's Meiring Naude Cruises. Part 16. Brachiopoda from the 1975-1979 cruises. *Annals of the South African Museum*, 97 (5), 97–140.
Hoffmann, J., Klann, M. & Matz, F. (2009) Recent thecideide brachiopods from the northern Great Barrier Reef, Australia (SW Pacific Ocean). *Zoosystematics and Evolution*, 85 (2), 341–349.
http://doi.org/10.1002/zoos.200900010
Hoffmann, J. & Lüter, C. (2009) Shell development, growth and sexual dimorphism in the Recent thecideide brachiopod *Thecidellina meyeri* sp. nov. from the lesser Antilles, Caribbean. *Journal of the Marine Biological Association of the United Kingdom*, 89 (3), 469–479.
http://doi.org/10.1017/s0025315409002616
Hoffmann, J. & Lüter, C. (2010) Shell development in thecidellinine brachiopods with description of a new Recent genus. *Special Papers in Palaeontology,* 84, 137–160.
International Commission on Zoological Nomenclature (1999) *International Code of Zoological Nomenclature*. *4th Edition*. International Trust for Zoological Nomenclature, London, 306 pp.
Lee, D.E. & Robinson, J.H. (2003) *Kakanuiella* (gen. nov.) and *Thecidellina*: Cenozoic and Recent thecideide brachiopods from New Zealand. *Journal of the Royal Society of New Zealand*, 33 (1), 341–361.
http://doi.org/10.1080/03014223.2003.9517734
Logan, A. (1988) A new thecideid genus and species (Brachiopoda, Recent) from the southeast North Atlantic. *Journal of Palaeontology*, 62, 546–551.
http://doi.org/10.1017/s0022336000018746

Logan, A. (2005) A new lacazelline species (Brachiopoda, Recent) from the Maldive Islands, Indian Ocean. *Systematics and Biodiversity*, 3 (1), 97–104.
http://doi.org/10.1017/s1477200004001586
Logan, A. (2008) Holocene thecideide brachiopods from the north-western Pacific Ocean: systematics, life habits and ontogeny. *Systematics and Biodiversity*, 6 (3), 405–413.
http://doi.org/10.1017/s1477200008002739
Logan, A. & Baker P. (2013) The development and shell microstructure of the pseudodeltidium and interarea in thecideide brachiopods. *Palaeontology*, 56 (2), 433–455.
http://doi.org/10.1111/pala.12001
Logan, A., Hoffmann, J. & Lüter, C. (2015) Checklist of Recent thecideoid brachiopods from the Indian Ocean and Red Sea, with a description of a new species of *Thecidellina* from Europa Island and a re-description of *T. blochmanni* Dall from Christmas Island. *Zootaxa*, 4013 (2), 225–234.
http://doi.org/10.11646/zootaxa.4013.2.4
Logan, A. & Zibrowius, H. (1994) A new genus and species of rhynchonellid (Brachiopoda, Recent) from submarine caves in the Mediterranean Sea. *Pubblicazioni della Stazione Zoologica di Napoli I—Marine Ecology*, 15 (1), 77–88.
http://doi.org/10.1111/j.1439-0485.1994.tb00043.x
Lüter, C., Hoffmann, J. & Logan, A. (2008) Cryptic speciation in the Recent thecideide brachiopod *Thecidellina* in the Atlantic and the Caribbean. *Earth and Environmental Science Transactions of the Royal Society of Edinburgh,* **98**, 405–413.
http://doi.org/10.1017/s1755691007078449
Lüter, C., Wörheide, G. & Reitner, J. (2003) A new thecideid genus and species (Brachiopoda, Recent) from submarine caves of Osprey Reef (Queensland Plateau, Coral Sea, Australia). *Journal of Natural History*, 37, 1423–1432.
http://doi.org/10.1080/00222930110120971
Muir-Wood, H.M. (1959) Report on the Brachiopoda of the John Murray Expedition. *John Murray Expedition Scientific Report*, 10 (6), 283–317.
Munier-Chalmas, E.P. (1880) Note sommaire sur les genres de la famille des Thecideidae. *Bulletin de la Société Géologique de France*, Série 3, 8, 279–280.
Pajaud, D. (1970) Monographie des Thécidées. *Mémoires de la Société géologique de France, Nouvelle Série*, 49 (112), 1–349.
Simon, E. (2010) *Argyrotheca furtiva* n. sp. and *Joania arguta* (Grant, 1983) two micromorphic megathyrid brachiopods (Terebratulida, Megathyridoidea) from the Indonesian Archipelago. *Bulletin de l'Institut royal des Sciences naturelles de Belgique, Biologie*, 80, 277–295.
Simon, E. & Hoffmann, J. (2013) Discovery of Recent thecideide brachiopods (Order: Thecideida, Family: Thecideidae) in Sulawesi, Indonesian Archipelago, with implications for reproduction and shell size in the genus *Ospreyella*. *Zootaxa*, 3694 (5), 401–433.
http://doi.org/10.11646/zootaxa.3694.5.1
Simon, E. & Willems, G. (1999) *Gwynia capsula* (Jeffreys, 1859) and other Recent brachiopods from submarine caves in Croatia. *Bulletin de l'Institut royal des Sciences naturelles de Belgique*, *Biologie*, 69, 15–21.
Simon, E., Logan, A., Zuschin, M., Mainguy, J. & Mottequin, B. (2016) *Lenticellaria* and *Hillerella*, new kraussinoid genera (Kraussinoidea, Brachiopoda) from Indo-Pacific and Red Sea waters: evolution in the subfamily Megerliinae. *Zootaxa*, 4137 (1), 1–34.
http://doi.org/10.11646/zootaxa.4137.1.1
Simon, E., Lüter, C., Logan, A. & Mottequin, B. (2018a) Recent thecideide brachiopods (Thecideida, Thecideoidea) from Indonesia with first discovery of a new *Thecidellina* species (Thecidellinidae), confirmed by molecular analyses. *Zootaxa*, 4526 (4), 481–515.
http://doi.org/10.11646/zootaxa.4526.4.4
Simon, E., Motchurova-Dekova, N. & Mottequin, B. (2018b) A reappraisal of the genus *Tethyrhynchia* Logan *in* Logan & Zibrowius, 1994 (Rhynchonellida, Brachiopoda), and a conflict between phylogenies obtained by morphological characters and molecular results. *Zootaxa*, 4471 (3), 535–555.
http://doi.org/10.11646/zootaxa.4471.3.6
Thomson, J.A. (1915) A new genus and species of Thecidiinae. *Geological Magazine*, New Series, Decade VI, 2, 461–464.
https://doi.org/10.1017/S0016756800203531
Williams, A., Carlson, S.J., Brunton, C.H.C., Holmer, L.E. & Popov, L. (1996) A supra-ordinal classification of the Brachiopoda. *Philosophical Transactions of the Royal Society of London*, B, 351 (4), 1171–1193.
http://doi.org/10.1098/rstb.1996.0101
Zezina, O.N. (1985) *Sovremennyie brachiopodi I Problemii bathalnoi zonii Okeana. [Contemporary brachiopods and the problems of the bathyal zone of the ocean]*. Isdatelistvo Nauka (ed.), Moscow, 247 pp. [in Russian]
Zezina, O.N. (1987) Brachiopods collected by BENTHEDI-Cruise in the Mozambique Channel. *Bulletin du Muséum d'Histoire naturelle*, Série 4, 9 (A3), 551–563.
Zezina, O.N. (1994) Recent brachiopods from underwater rises of the Western part of the Indian Ocean. *Trudy Instituta Okeanologii Akademii Nauk SSSR*, 129, 44–52. [in Russian]
Zumwalt, G.S. (1970) *The functional morphology of the tropical brachiopod* Thecidellina congregata *Cooper, 1954*. Unpublished MS Thesis, University of California, Davis, 135 pp. [*non vidi;* cited in Hoffmann & Lüter, 2009]

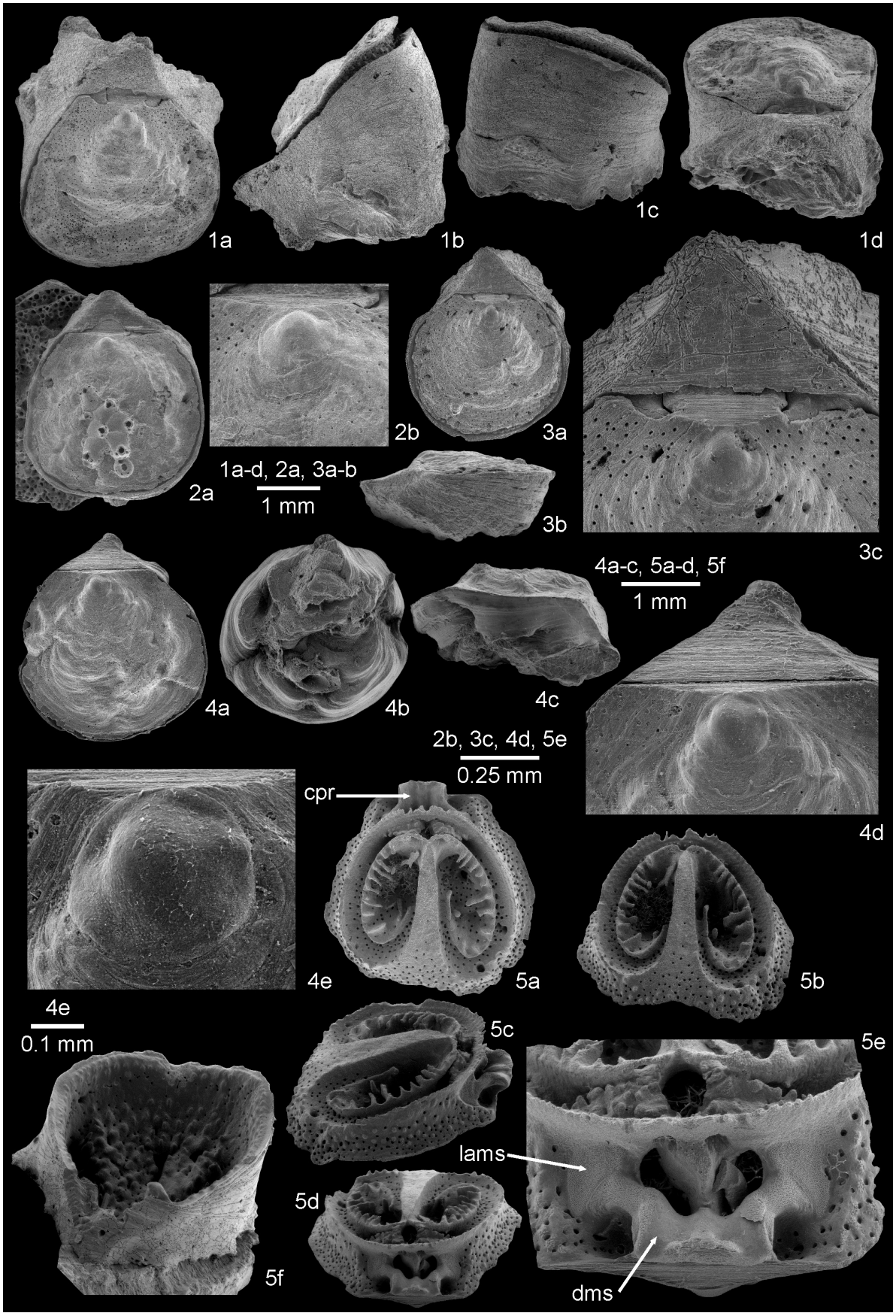
1a
1b
1c
1d
2a
2b
3a
1a-d, 2a, 3a-b
1 mm
3b
3c
4a-c, 5a-d, 5f
1 mm
4a
4b
4c
2b, 3c, 4d, 5e
0.25 mm
4d
cpr
4e
5a
5b
4e
0.1 mm
5c
5e
lams
5d
5f
dms

PLATE1.

PLATE 1. *Thecidellina leipnitzae* **sp. nov.**, "La Passe bateau" off the south-west coast of Mayotte Island.
Fig. 1a–d. MNHN-IB-2017-157 (paratype), large adult articulated specimen in dorsal, lateral, anterior and posterior views.
Fig. 2a–b. MNHN-IB-2017-158 (paratype), adult articulated specimen fixed on a bryozoan shell in dorsal view and detailed view of the protegulum with its granular surface.
Fig. 3a–c. MNHN-IB-2017-159 (paratype), adult articulated specimen in dorsal and lateral views, and detailed view of the interarea.
Fig. 4a–e. MNHN-IB-2017-160 (paratype), articulated specimen in dorsal, ventral and lateral views, detailed view of the pointed triangular ventral interarea, and close-up of the protegulum with its granular surface.
Fig. 5a–f. MNHN-IB-2017-161 (paratype). a–e. Dorsal valve with developed brachial cavities in internal (cpr = cardinal process), oblique anterior, oblique semi-lateral and posterior views, and detailed view of the posterior part (lams = lateral adductor muscle scar, dms = diductor muscle scar). f. Ventral valve in oblique postero-dorsal view.

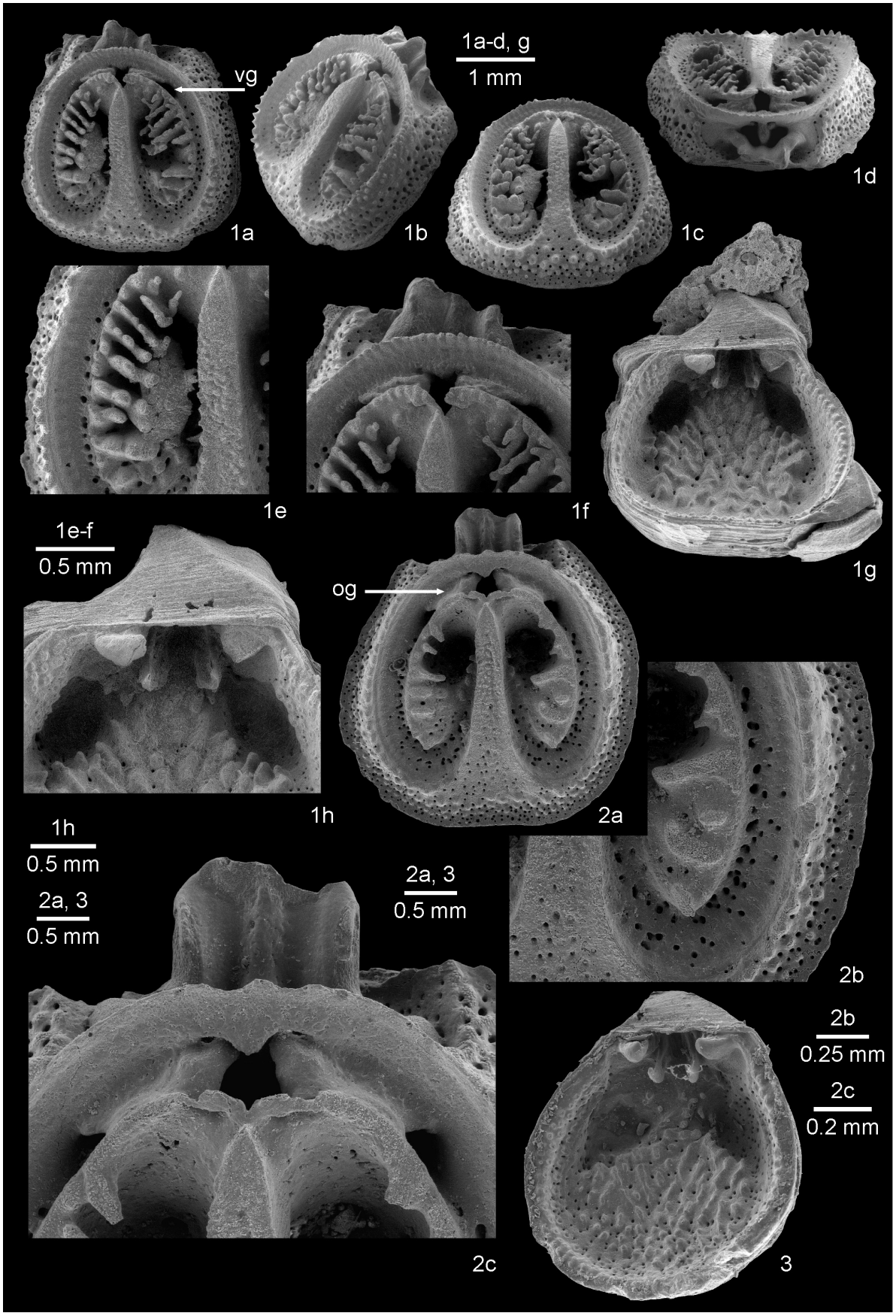
vg
1a-d, g
1 mm
1a
1b
1c
1d
1e
1f
1g
1e-f
0.5 mm
og
1h
2a
2b
1h
0.5 mm
2a, 3
0.5 mm
2a, 3
0.5 mm
2b
0.25 mm
2c
0.2 mm
2c
3

PLATE 2.

PLATE 2. *Thecidellina leipnitzae* **sp. nov.**, "La Passe bateau" off the south-west coast of Mayotte Island.
Fig. 1a–h. MNHN-IB-2017-162 (holotype), adult specimen opened for studying the internal structures. a–f. Dorsal valve interior in plan (vg = visceral gap), oblique lateral, oblique anterior and oblique posterior views, detailed view of the flat septum surface and of the canopying spicules (at this high magnification it is possible to see the granular ornamentation of their ventral edges) and close-up of the posterior part of the valve showing the pointed end of the septum, the small orifices and the posterior outgrowths joining the intrabrachial ridge to the brachial bridge (the structure of the trilobed cardinal process is visible (partly broken when opening the shell)). g–h, ventral interior in plan view and detailed view of the interarea, of the teeth, of the hemispondylium made of two subparallel prongs with pointed tips and of the gonad pits.
Fig. 2a–c. MNHN-IB-2017-163 (paratype), dorsal valve interior of a peculiar specimen with reduced brachial cavities in plan view (og = posterior outgrowth), detailed view of the fused spicules forming the anterior part of the canopy and of the wide anterior part of the septum (the ventral edges of the spicules have a granular surface), and close-up of the posterior part of the valve (the pointed end of the septum is visible as are the strong posterior outgrowths; the thick median lobe of the cardinal process is clearly visible).
Fig. 3. MNHN-IB-2017-164 (paratype), ventral valve in oblique anterior dorsal view, illustrating the teeth, hemispondylium, smooth gonad pits and rough tubercles on the valve floor.

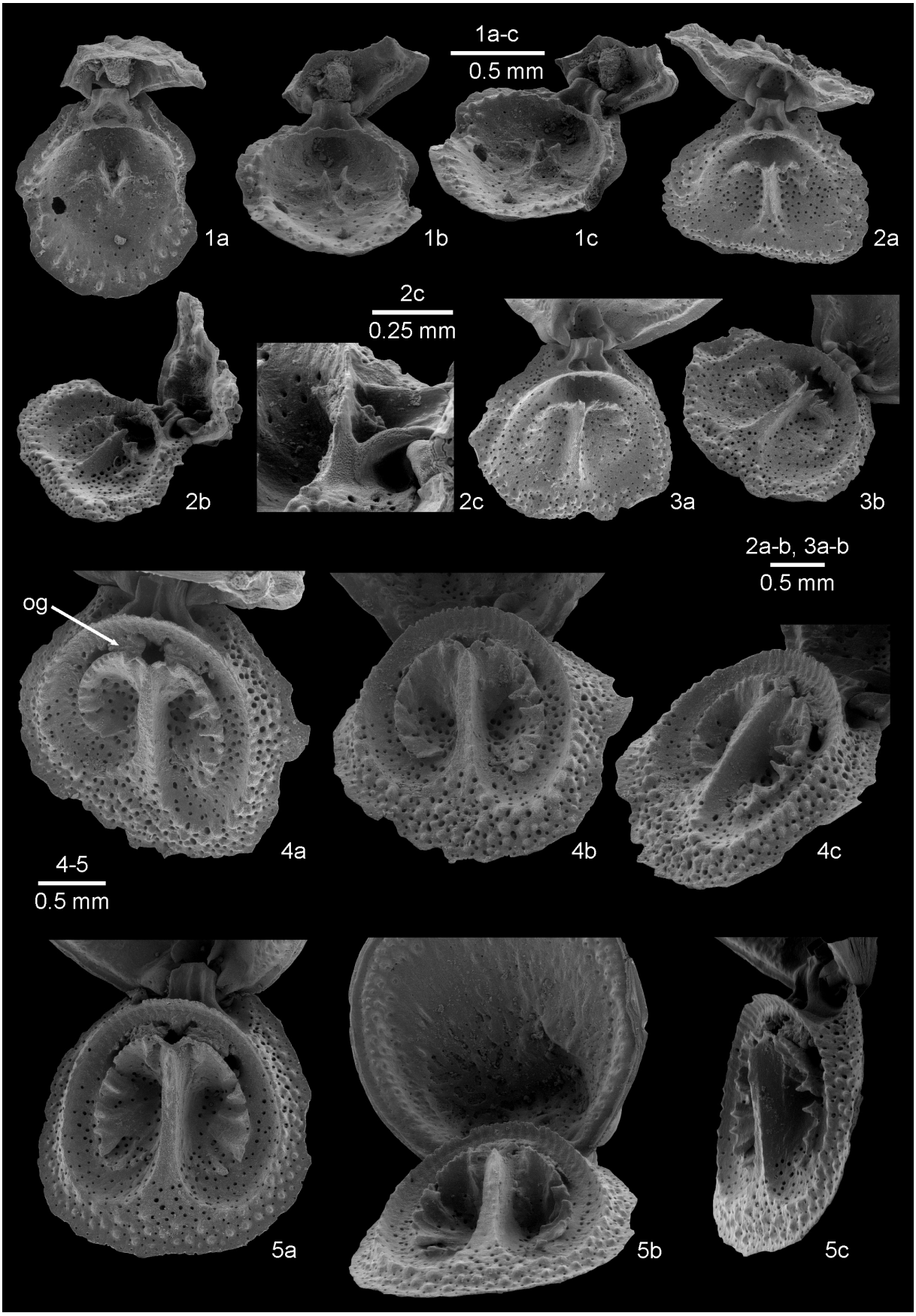
1a-c
0.5 mm
1a
1b
1c
2a
2c
0.25 mm
2b
2c
3a
3b
2a-b, 3a-b
0.5 mm
og
4a
4b
4c
4-5
0.5 mm
5a
5b
5c

PLATE 3.

PLATE 3. *Thecidellina leipnitzae* **sp. nov.**, "La Passe bateau" off the south-west coast of Mayotte Island.
Fig. 1a–c. MNHN-IB-2017-165 (paratype), interior of an early juvenile articulated specimen (showing the central spikes with pointed tips oriented backwards, the first stage of growth of the posterior part of the intrabrachial ridge and the complete brachial bridge) in plan, oblique anterior (the septum is emerging and is fused with the anterior base of the central spikes; some nodules (or small tubercles) which are the beginning of the construction of the brachial cavities are visible) and semi-oblique lateral views.
Fig. 2a–c. MNHN-IB-2017-166 (paratype), interior of a juvenile articulated specimen (showing a more developed intrabrachial ridge and a stronger dorsal septum which still has a concave ventral edge; the calcitic pole is already developed) in plan (the cardinal process and the ventral hemispondylium are intact) and oblique semi-lateral views (the height of the septum at this stage of growth is already very important), and detailed view of the hinge at this stage of growth (there is already secondary shell material on the side of the cardinal process).
Fig. 3a–b. MNHN-IB-2017-167 (paratype), interior of an articulated specimen in plan (showing the septum better developed as are the brachial cavities) and oblique semi-lateral views (showing clearly the individual plates building the brachial cavities).
Fig. 4a–c. MNHN-IB-2017-168 (paratype), interior of an articulated young specimen in plan (the brachial cavities are nearly complete except in their anterior part; the canopying spicules are developed on each plate that constructed the intrabrachial ridge; the posterior outgrowths (og) are completely developed), oblique anterior (the ventral edge of the dorsal septum is becomes flatter as it is progressively filled with new shell material; the peripheral ridge bears more tubercles), and oblique lateral views giving a better view of the structure of the dorsal septum.
Fig. 5a–c. MNHN-IB-2017-169 (paratype), interior of a nearly complete adult articulated specimen in plan (the brachial cavities are nearly complete, and the spicules of the canopy are emerging but are far from being totally developed; the marsupial orifices are clearly visible as are the posterior outgrowths), oblique anterior (showing the individual plates that are the basement of the intrabrachial ridge and each bearing one spicule in development; the dorsal septum is now completely developed) and oblique semi-lateral views (showing clearly the development of the internal lateral parts of the brachial cavities; in their posterior part secondary material is added against the lateral parts of the septum).

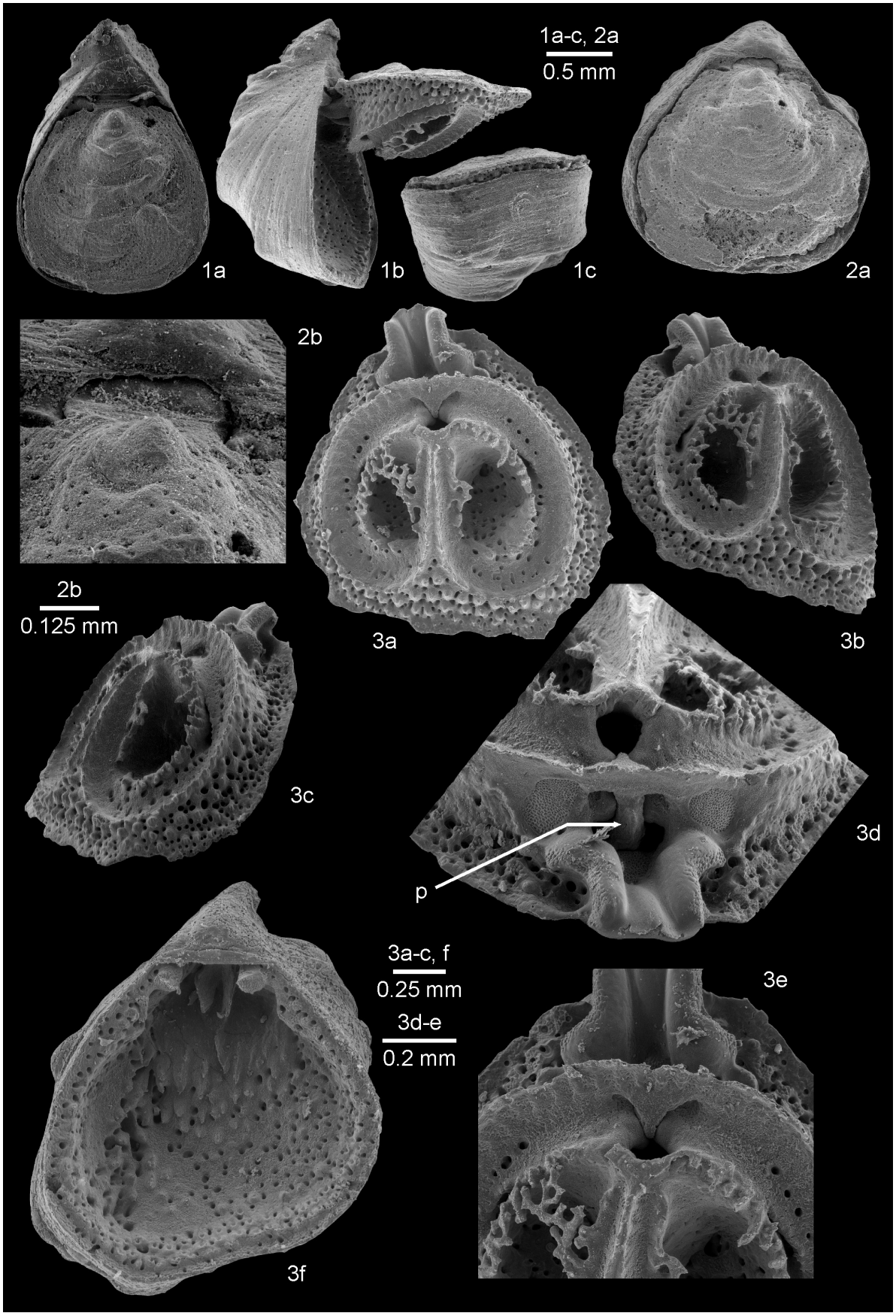
1a-c, 2a
0.5 mm
1a
1b
1c
2a
2b
2b
0.125 mm
3a
3b
3c
3d
p
3a-c, f
0.25 mm
3d-e
0.2 mm
3e
3f

PLATE 4.

PLATE 4. *Minutella* cf. *minuta* (Cooper, 1981), "La Passe bateau" off the south-west coast of Mayotte Island.
Fig. 1a–c. MNHN-IB-2017-170, large articulated adult specimen in dorsal, lateral (showing the dorsal and ventral internal structure), and posterior views.
Fig. 2a–b. MNHN-IB-2017-171, adult articulated specimen in dorsal view and detailed view of the straight hinge and of the anterior part of the rugideltidium (the protegulum is clearly visible and it is well limited by a step like growth line).
Fig. 3a–f. MNHN-IB-2017-172, adult specimen. a-e. Dorsal interior in plan, antero-lateral oblique, oblique lateral views, detailed view of the posterior part of the dorsal valve (the posterior visceral gap through the intrabrachial ridge and the marsupial orifices are clearly visible; the calcitic pole is thick but remains free from the dorsal valve floor; the lateral adductor muscle scars are semicircular to kidney-shaped and they are placed on either side of the visceral gap), close-up of the posterior part showing the calcitic pole (p) bearing an excrescence, and detailed view of the anterior part of the cardinal process. f. Ventral interior in plan view.

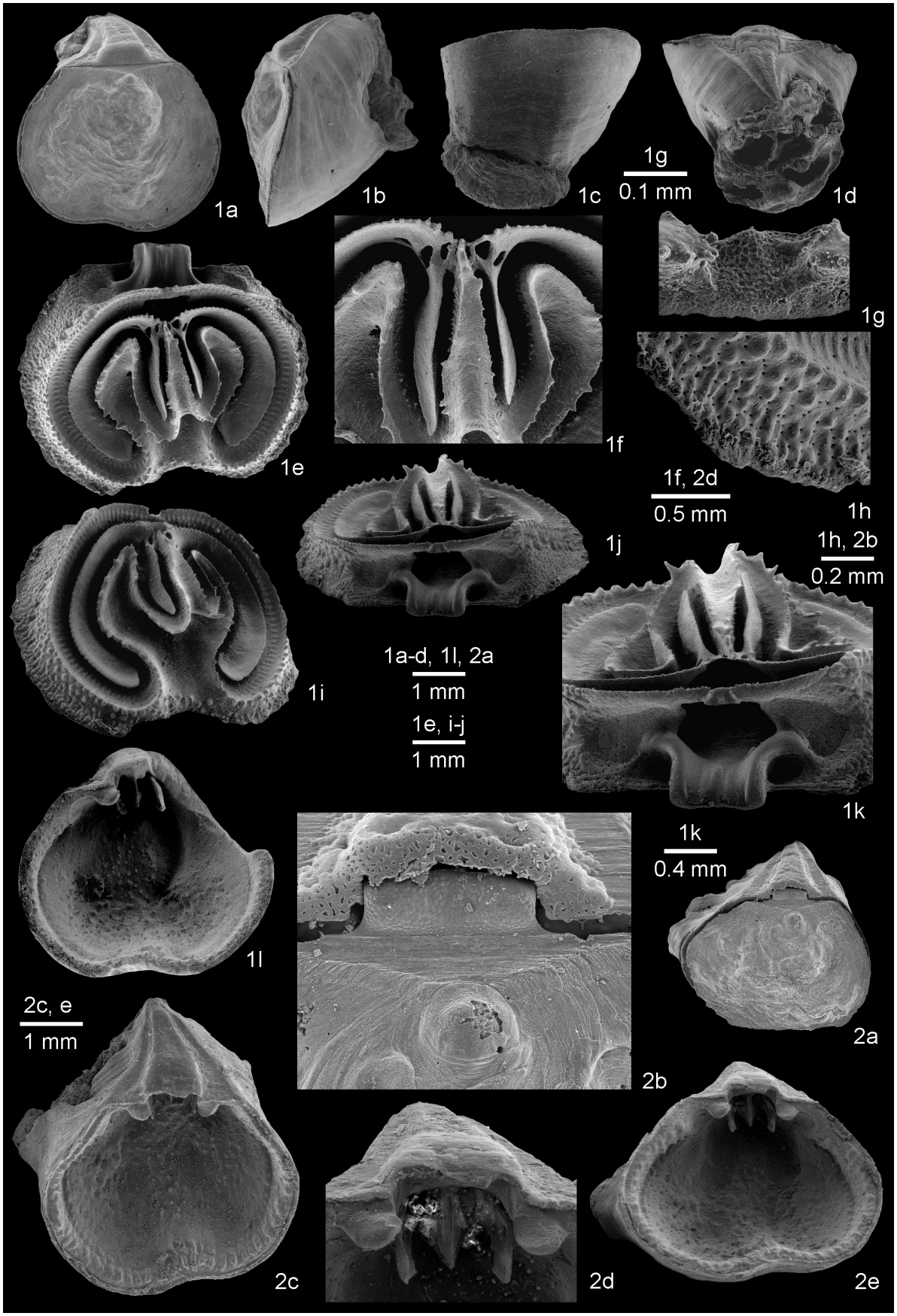
1a
1b
1c
1g
0.1 mm
1d
1g
1f
1e
1f, 2d
0.5 mm
1h
1h, 2b
0.2 mm
1j
1a-d, 1l, 2a
1 mm
1e, i-j
1 mm
1i
1k
1k
0.4 mm
1l
2a
2c, e
1 mm
2b
2c
2d
2e

PLATE 5.

PLATE 5. *Ospreyella mayottensis* **sp. nov.**, "La Passe bateau" off the south-west coast of Mayotte Island.
Fig. 1a–l. MNHN-IB-2017-179 (holotype). a–d. Articulated adult specimen (female) in dorsal, lateral, anterior and posterior views. e–k. Dorsal interior in plan view, close-up of the median ramus attached to the jugum which connects also the major interbrachial lobes (detailed view of the minor interbrachial lobes which are straight and never furcated), detailed view of the marsupial notch, detailed view of the peripheral rim with tubercles having a tip bearing small radial ridges (the endopunctae are rather small), oblique anterior view showing the median depression and a complete view of the *apparatus ascendens*, posterior view showing the height of the median ramus, detailed view of the posterior part of the dorsal valve (lateral adductor muscle scars are easily seen as is the structure of the cardinal process). l. Ventral interior in plan view showing the spiny floor and the low median ridge.
Fig. 2a–e. MNHN-IB-2017-180 (paratype). a–b. Articulated specimen in dorsal view and close-up of dorsal umbo with the interarea and the convex rugideltidium. c–e. Ventral interior in plan view, detailed view of the teeth and of the hemispondylium, and anterior oblique view showing the hemispondylium and the median ridge on the valve floor.

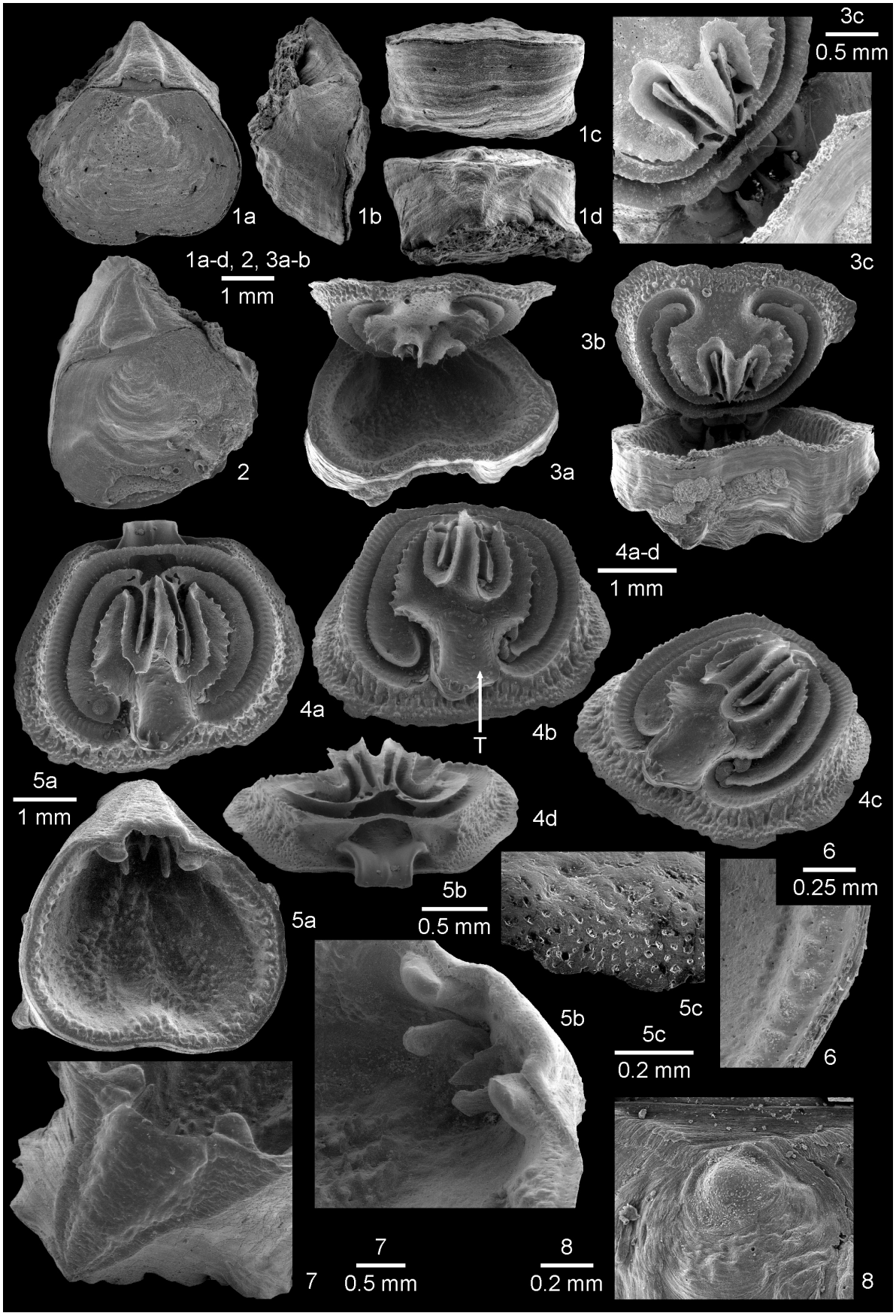
1a
1b
1c
1d
1a-d, 2, 3a-b
1 mm
3c
0.5 mm
3c
2
3a
3b
4a-d
1 mm
4a
T
4b
4c
4d
5a
1 mm
5a
5b
0.5 mm
5b
5c
5c
0.2 mm
6
0.25 mm
6
7
0.5 mm
7
8
0.2 mm
8

PLATE 6.

PLATE 6. *Ospreyella mayottensis* **sp. nov.**, "La Passe bateau" off the south-west coast of Mayotte Island.
Fig. 1a–d. MNHN-IB-2017-181 (paratype), large articulated adult specimen in dorsal, lateral, anterior and posterior views.
Fig. 2. MNHN-IB-2017-182 (paratype), articulated adult specimen in dorsal view.
Fig. 3a–c. MNHN-IB-2017-183 (paratype), complete articulated specimen opened to show the internal aspect of the dorsal and ventral valves in oblique anterior and anterior views, and close-up of the dorsal interior.
Fig. 4a–d. MNHN-IB-2017-184 (paratype), dorsal interior of an adult male specimen (after its death, a young *Thecidellina leipnitzae* **sp. nov.** (arrowed "T") attached and began its life in the median depression of the dorsal valve) in plan, anterior oblique, oblique antero-lateral and posterior views.
Fig. 5a–b. MNHN-IB-2017-185 (paratype), ventral interior in plan view, detailed view of the hemispondylium with the two lateral prongs and the median lamella, and the cyrtomatodont teeth, and close-up of the of the anterior perforated side of the rugideltidium.
Fig. 6. MNHN-IB-2017-186 (paratype), detailed view of the lateral commissure and of the tuberculate peripheral rim in a ventral valve.
Fig. 7. MNHN-IB-2017-187 (paratype), close-up of ventral interarea and the convex rugideltidium.
Fig. 8. MNHN-IB-2017-188 (paratype), dorsal valve, detailed view of protegulum.

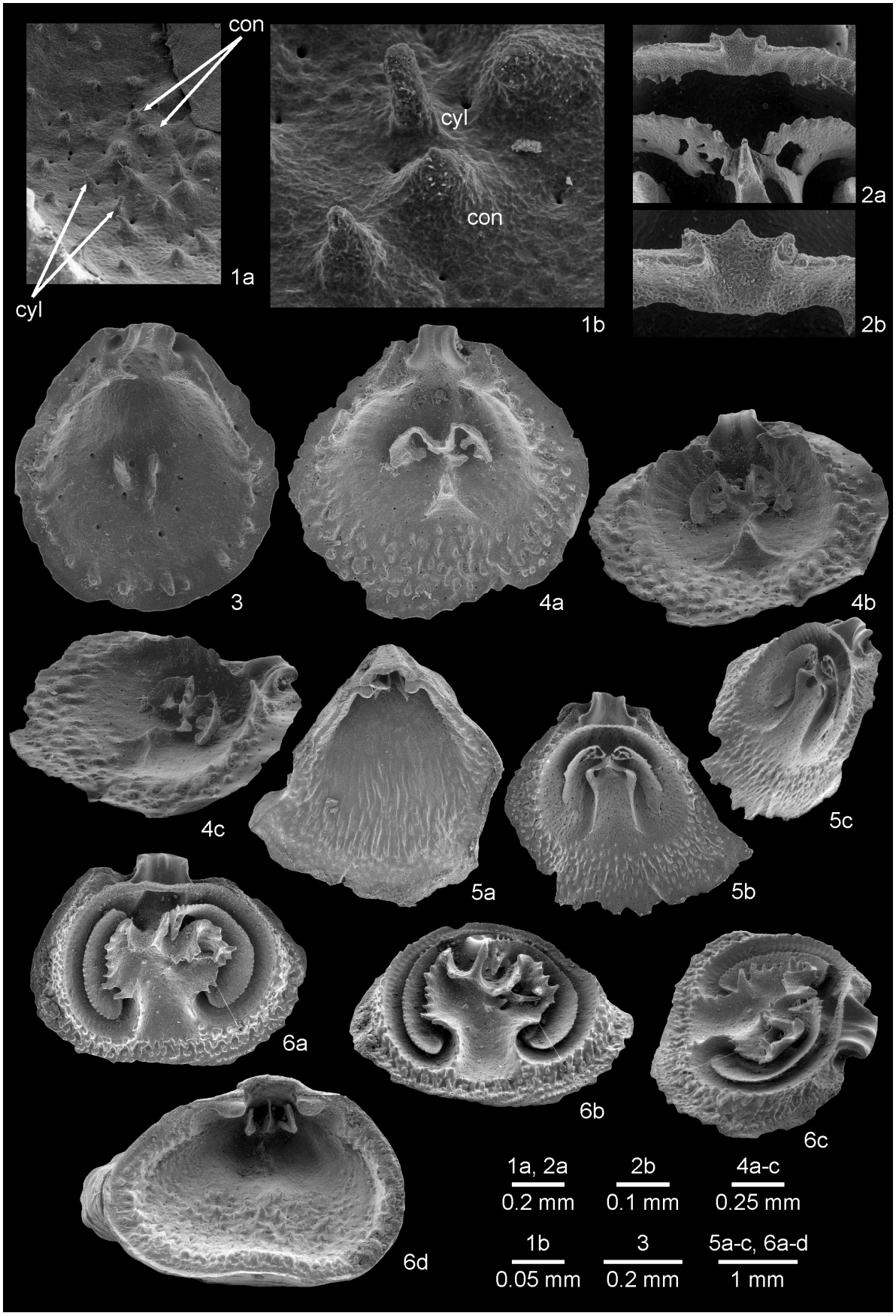
con
cyl
1a
cyl
con
1b
2a
2b
3
4a
4b
4c
5a
5b
5c
6a
6b
6c
6d
1a, 2a
0.2 mm
2b
0.1 mm
4a-c
0.25 mm
1b
0.05 mm
3
0.2 mm
5a-c, 6a-d
1 mm

PLATE 7.

PLATE 7. *Ospreyella mayottensis* **sp. nov.**, "La Passe bateau" off the south-west coast of Mayotte Island.
Fig. 1a–b. MNHN-IB-2017-189 (paratype), two detailed views of the ventral valve floor showing the spinous ornamentation made of two kinds of spine (thin, needle-like and with a cylindrical outline (cyl) and wider, conical spines (con).
Fig. 2a–b. MNHN-IB-2017-190 (paratype), detailed view of a female brachial bridge with a marsupial notch seen in anterior view (note the denticulate ventral edge of the brachial bridge) and close-up of the marsupial notch with its posterior lobe and with the muscle scars of the specialized tentacles.
Fig. 3. MNHN-IB-2017-191 (paratype), dorsal valve of an early juvenile specimen.
Fig. 4a–c. MNHN-IB-2017-192 (paratype), dorsal valve interior of a juvenile specimen in plan, oblique anterior and oblique lateral views.
Fig. 5a–c. MNHN-IB-2017-193 (paratype), a very young disarticulated specimen showing juvenile stage of growth for the ventral and dorsal valves. a. Ventral valve interior in plan view. b–c. Dorsal valve interior in plan and oblique lateral views.
Fig. 6a–d. MNHN-IB-2017-194 (paratype), a young disarticulated specimen. a–c. Dorsal valve interior in plan, oblique anterior and oblique lateral views. d. Ventral valve interior in oblique anterior view.